
Article:
Liu, Y. orcid.org/0000-0001-6893-3913, Yang, M., Ding, Y. et al. (2 more authors) (2022) Process modelling, optimisation and analysis of heat recovery energy system for petrochemical industry. Journal of Cleaner Production, 381. 135133. ISSN: 0959-6526

https://doi.org/10.1016/j.jclepro.2022.135133

Journal of Cleaner Production 381 (2022) 135133

Contents lists available at ScienceDirect

Journal of Cleaner Production

journal homepage: www.elsevier.com/locate/jclepro

Process modelling, optimisation and analysis of heat recovery energy system for petrochemical industry

Yurong Liu [a], Minglei Yang [a,c], Yuxing Ding [b], Meihong Wang [a,b,*], Feng Qian [a,c,d,**]

[a] Key Laboratory of Advanced Control and Optimisation for Chemical Processes, Ministry of Education, East China University of Science and Technology, Shanghai, 200237, China
[b] Department of Chemical and Biological Engineering, The University of Sheffield, Sheffield S1 3JD, United Kingdom
[c] Engineering Research Center of Process System Engineering, Ministry of Education, East China University of Science and Technology, Shanghai, 200237, China
[d] Shanghai Institute of Intelligent Science and Technology, Tongji University, Shanghai, 200092, China

ARTICLE INFO

Handling Editor: Cecilia Maria Villas Bôas de Almeida

Keywords:
Process optimisation
Waste heat recovery
Heat exchanger network
Organic rankine cycle
Petrochemical plant
Phase changing streams

ABSTRACT

The petrochemical industry is an energy-intensive process. Heat exchanger network (HEN) is widely applied in existing petrochemical plants used to save energy. However, there is still some amount of low-grade heat wasted. No mathematical model can directly tackle the problems with majority of phase-changing process streams. Therefore, this study aims to optimise an extended low-grade heat recovery model for the petrochemical plant by integrating the organic Rankine cycle (ORC) with HEN. A mixed-integer nonlinear programming steady-state model was first developed. Then, the ORC operation conditions were optimised simultaneously. Finally, the thermodynamics (energy and exergy) and economic analysis were performed to evaluate the system performance, with 41 MW more heat recovered, 2.01% higher exergy efficiency and 3219 k$/year less total annual cost, compared with HEN only. Furthermore, the optimisation results indicate that the proposed energy system performs with 386 MW of recovered heat from the process streams, 82.13% of the overall exergy efficiency, 3.94 MW of net power generated from ORC, and 4416 k$/year of electricity profit. Research presented in this paper hopes to shed light on design and operation of the petrochemical industry for energy savings and cost reduction.

1. Introduction

A petrochemical complex plant is a combination of process units that convert naphtha and pyrolysis gasoline into the basic petrochemical intermediates: benzene, toluene, and xylenes (BTX) (Meyers, 2004). The configuration of the petrochemical plant varies by plant. The basic configuration includes several units: a catalytic reforming unit, a disproportionation unit, an isomerisation unit, a parex unit, an extraction unit, and a xylene fractionation unit. This process comprises a series of reactions and separation operations involving various temperatures and pressures. It is highly energy-intensive (Chen et al., 2014). Distillation is one of the most commonly used separation procedures and the least energy-efficient (Shahandeh et al., 2014). Consequently, it is essential to research energy systems to increase energy efficiency. The heat exchanger network (HEN) is an efficient approach to recovering the heat, consequently improving the energy system performance. Several methodologies have been developed and effectively applied in the industry during the past few decades [4–14]. For the energy system of the petrochemical complex, Zhang et al. (2014) proposed a HEN model based on the transshipment model (Papoulias and Grossmann, 1983a, 1983b, 1983c) to reduce the utility requirements for a toluene disproportionation unit. Psaltis et al. (2016) developed a framework to optimise the process integration synthesis problem based on the HEN model presented by Ponce-Ortega et al. (2008). They applied it to the disproportionation and xylene fractionation units. Liu et al. (2021) developed a framework to optimise the process and HEN models for isomerisation, parex, and xylene fractionation units.

However, in these papers, the streams associated with the low-temperature heat source in the petrochemical complex were directly cooled using the cold utility. None of these studies examined the possibility of expanding the use of these low-temperature hot streams. Based on these conditions, research challenges arise from the need further to enhance the heat utilisation of the petrochemical plant. The

* Corresponding author. Mappin Street, Sheffield, S1 3JD, United Kingdom.
** Corresponding author. No.130 MeiLong Rd, Shanghai, 200237, PR China.
E-mail addresses: y11180383@mail.ecust.edu.cn (Y. Liu), mlyang@ecust.edu.cn (M. Yang), yding32@sheffield.ac.uk (Y. Ding), Meihong.Wang@sheffield.ac.uk (M. Wang), fqian@ecust.edu.cn (F. Qian).

https://doi.org/10.1016/j.jclepro.2022.135133
Received 31 July 2022; Received in revised form 25 September 2022; Accepted 7 November 2022
Available online 12 November 2022

Abbreviations

BTX	benzene, toluene, and xylenes
HEN	heat exchanger network
ORC	Organic Rankine cycle
MINLP	mixed-integer nonlinear programming
3E	energy, exergy, and economic
C8A	C8 aromatic isomers
PX	para-xylene
OX	ortho-xylene
C8A+	C8 + aromatics
HE	heat exchanger
T-S	temperature-entropy
SWS	stage-wise superstructure
MSWS	modified stage-wise superstructure
CMA-ES	covariance matrix adaptation evolution strategy

Nomenclature

S	stream
R	reactor
SP	splitter
D	distillation column
H	hot stream
C	cold stream

Parameters

AF	annual factor
$t_{working}$	working hours (h)
C	fixed cost ($)
α	parameter for the equipment
i	fractional interest rate per year
n	horizon time

Variables

$\dot{Q}$	heat flow (kW)
m	mass flow (kg/s)
h	enthalpy (kJ/kg)
$\dot{W}$	work (kW)
η	efficiency
$\dot{E}xg$	exergy rate (kW)
s	entropy ($kJ/^{\circ}C$)
$\dot{L}$	exergy destruction (kW)
TAC	total annual cost ($k\$/year$)
COP	cost of equipment ($k\$/year$)
$Utility$	cost of utility ($k\$/year$)
ELE	profit of electricity ($k\$/year$)
$Costhc$	cost of heat exchanger ($k\$/year$)
$Costcu$	cost of cooler ($k\$/year$)
$Costhu$	cost of heater ($k\$/year$)
$Areahc$	area for the heat exchanger (m^2)
$Areacu$	area for the cooler (m^2)
$Areahu$	area for the heater (m^2)
qcu	heat load for cooler (kW)
qhu	heat load for heater (kW)
z	binary variable to select the heat exchanger
zhu	binary variable to select the heater
zcu	binary variable to select the cooler

Superscripts

Rec	recovery
HE	heat exchanger
ORC	ORC sub-system
$heater$	heater
$cooler$	cooler
HEN	HEN sub-system
$ovrl$	overall

Subscripts

eva	evaporator
tur	turbine
con	condenser
$pump$	pump
wf	working fluid
net	net value
ene	energy
0	atmospheric conditions (25 °C, 1atm)
ph	process hot stream
pc	process cold stream
Exg	exergy
hu	hot stream
cu	process cold stream
oh	ORC hot stream
oc	ORC cold stream
k	stage

low-temperature heat recovery in the petrochemical complex is studied in this paper.

In contrast, many industrial operations generate enormous amounts of waste heat. It was caused by inefficient equipment and operations, and thermodynamic constraints on equipment and processes (Reddy et al., 2013). For example, in a distillation column, the overhead streams at temperatures of 100–200 °C reject heat by fin-fan coolers, and streams at a temperature less than 100 °C reject heat to the cooling water system. Thus, the heat in these low-temperature streams is wasted. Industrial waste heat accounted for 10%–50% of total fuel consumption in various industrial sectors (Chen et al., 2016b). Therefore, there is a great potential to recover the waste heat. Organic Rankine cycle (ORC) is one of the promising technologies to convert low-temperature heat into electricity. It is analogous to the Rankine cycle for steam but employs organic substances such as hydrocarbons or refrigerants. Compared with water, these organic substances boil at lower temperatures and pressure. There are several advantages to using organic working fluid, including long service life, low maintenance requirements, and utilising waste heat at various temperatures (Kermani et al., 2018). In addition to ORCs, Kalina and trilateral Rankine cycles have been intensively studied. Yari et al. (2015) compared these three cycles from thermodynamic and exergoeconomics and found that ORC is the most advantageous from an economic standpoint. ORC is a mature technology and commercially available in many fields, including solar thermal energy (Boyaghchi and Heidarnejad, 2015; Bruno et al., 2008; Cioccolanti et al., 2019; Freeman et al., 2015; Sonsaree et al., 2018), geothermal energy (Altun and Kilic, 2020; Aneke et al., 2011; DiPippo, 2012; Ghasemi et al., 2013; Gökgedik et al., 2016), engine waste heat recovery (Daghigh and Shafieian, 2016; Hoang, 2018; Horst et al., 2013; Lion et al., 2020; Ringler et al., 2009), biomass energy (Algieri and Morrone, 2012; Drescher and Brüggemann, 2007; Maraver and Royo, 2017; Świerzewski and Kalina, 2020; Tańczuk and Ulbrich, 2013), and industrial waste heat (Aneke et al., 2012; Campana et al., 2013; Fergani et al., 2016; Kaşka, 2014; Moreira and Arrieta, 2019; Ding et al., 2022; Liu et al., 2022).

However, few studies focus on waste heat recovery for a refinery (Chen et al., 2016a; Jung et al., 2014; Mehdizadeh-Fard and Pourfayaz, 2019; Song et al., 2014), and these studies are still at the research stage and not yet widely adopted. None of the mentioned papers investigates waste heat utilisation in a petrochemical plant. In summary, the current applied energy system for the petrochemical industry uses HEN without

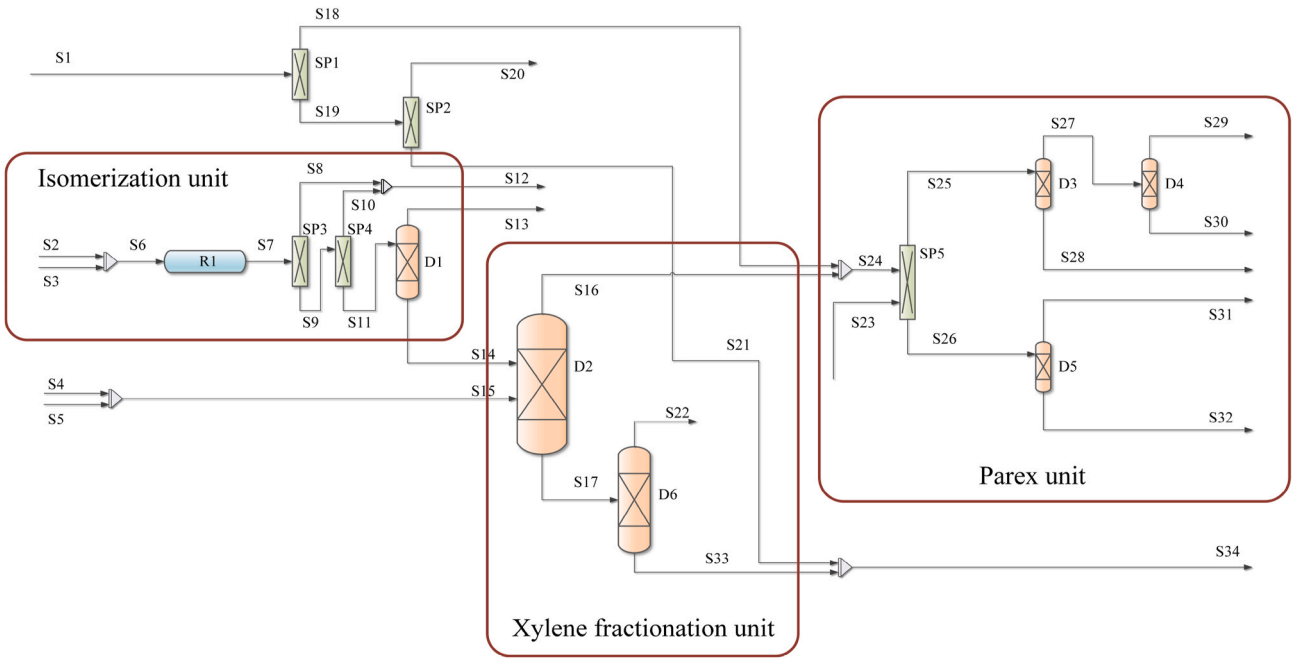

Note: The capital letters S, R, SP, and D represent stream, reactor, splitter, and distillation column, respectively.

Fig. 1. Process flow diagram of the investigated petrochemical plant (Liu et al., 2021). Note: The capital letters S, R, SP, and D represent stream, reactor, splitter, and distillation column, respectively.

addressing low-temperature heat. The ORC system has strong advantages for recovering low-temperature heat. Thus, research challenges arise from designing an ORC system for the existing HEN in the petrochemical complex plant. This study aims to optimise an extended low-grade heat recovery model for the petrochemical plant by integrating the ORC with HEN. A mixed-integer nonlinear programming (MINLP) model was developed, and a decomposed strategy was applied to solve the model. Then, the ORC operating conditions and heat recovery system configuration were simultaneously optimised. Finally, thermodynamics (energy and exergy) and economic (3E) assessment (Adibhatla and Kaushik, 2017) were used to evaluate the performance of the proposed heat recovery system. The following are the novel contributions of this research:

- A new scheme for a low-grade heat recovery system in a petrochemical plant was proposed.
- Mixed-integer nonlinear programming (MINLP) model was developed for the suggested steady-state system.
- The decomposed strategy was applied to solve the medium-scale HEN problem, which includes the majority of phase changing streams.
- The operation conditions of ORC (evaporation temperature, condensation temperature, and the mass flow of ORC working fluid) and the system configuration were optimised simultaneously.
- For the optimal low-grade heat recovery system, detailed thermodynamics (energy and exergy) and economic analyses were investigated to evaluate the system's performance.

The rest of this paper is structured as follows. Section 2 describes the petrochemical plant and the detailed process, followed by the mathematic models and performance analysis methodologies presented in Section 3. Then, the thermodynamics and economic analysis of the proposed system are discussed, and the optimal operating conditions of the proposed system are given. Finally, conclusions are drawn in Section 5.

2. Process description of the heat recovery system for the petrochemical plant

2.1. Process description and simulation of the petrochemical plant

For the petrochemical plant, the investigated process contains: isomerisation, parex, and xylene fractionation. The process flow diagram is shown in Fig. 1 (Liu et al., 2021). In the isomerisation unit, it contains a reactor (R1), a deheptanizer column (D1), and two splitters (SP3 and SP4). The main function is to convert C8 aromatic isomers (C8A) into para-xylene (PX). The lean PX solution (S2) and hydrogen (S3) are feedstocks to R1. The function of two splitters (SP3 and SP4) is to eliminate hydrogen from the overheads. Then, the effluent (S11) is sent to D1 to remove heptane from the column overhead. The bottom (S14) is sent to the xylene fractionation unit.

The xylene fractionation unit contains two distillation columns, named xylene splitter (D2) and the ortho-xylene (OX) column (D6), respectively. The feeds of D2 are from two streams (S14 and S15) and consist of C8+ aromatics (C8A+). The D2 effluent (S17) is sent to D6, where a high-purity OX product (S22) is obtained. The D6 effluent (S33) is usually blended into gasoline or fuel oil.

The Parex unit contains one splitter (SP5) and three distillation columns, named the extraction column (D3), the finishing column (D4), and the raffinate column (D5), respectively. The process is to purify the final product PX. The feed is the mixture of D2 overhead (S16) and C8A from the disproportionation unit (S1). S23 is the desorption agent consisting of p-diethylbenzene. In SP5, PX is extracted by adsorptive separation first. Then, the overhead (S25) is the extracted solution sent to D3,

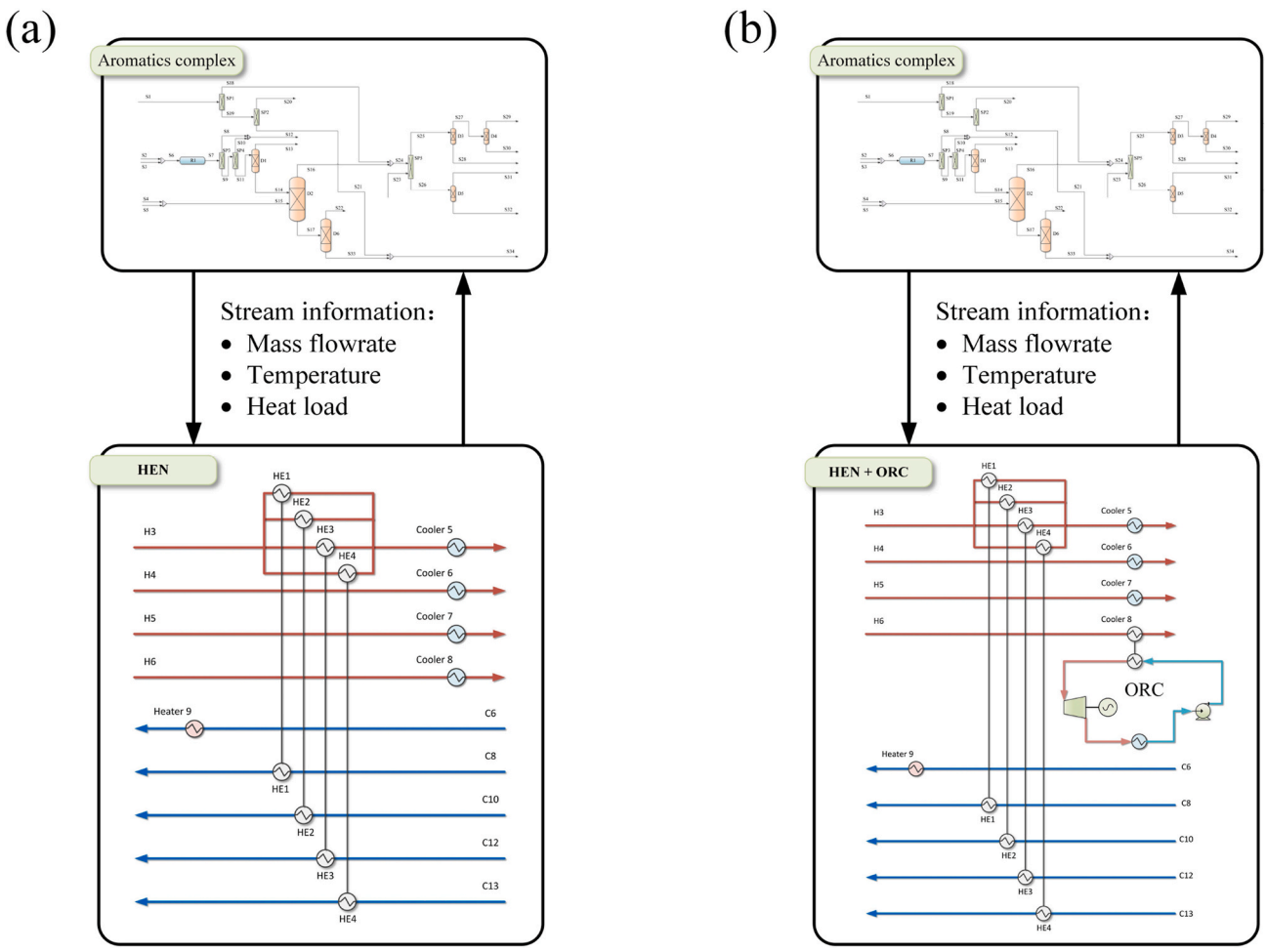

Fig. 2. The energy system of the petrochemical plant (a) with HEN (Liu et al., 2021) and (b) with both HEN and ORC.

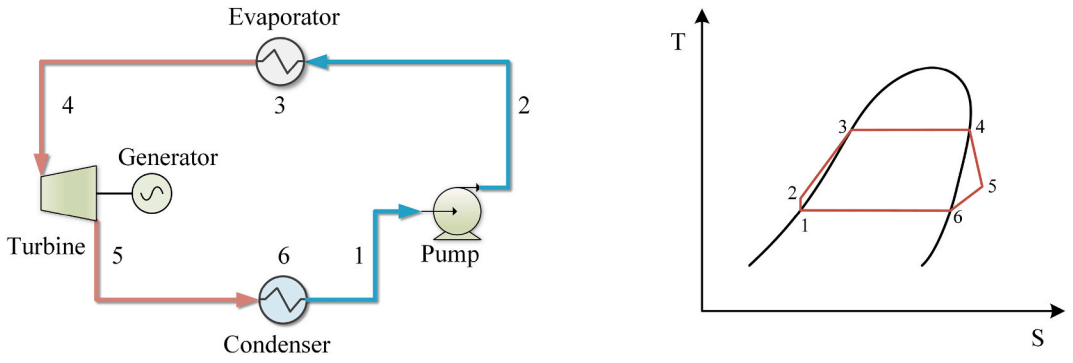

Fig. 3. The flowsheet and T-S diagram of a typical ORC.

while the bottom is the remaining extracted solution sent to D5. S28 and S32, the effluents from D3 and D5, are almost completely depleted of PX. The D5 overhead (S31) is the lean PX solution. Finally, the pure product PX (S30) is recovered from the D4 bottom.

The petrochemical plant was simulated in Aspen HYSYS at steady state condition. The detailed feed composition, operation conditions and design specifications of the distillation columns, and reactor operation conditions were the same as described in the published literature (Liu et al., 2021). The stream data in the proposed heat recovery system was obtained from the HYSYS model, including the supply and target temperatures, flow rates, and heat loads.

2.2. Heat recovery system (HEN and ORC) for the petrochemical plant

The HEN can recover heat from distillation columns, particularly the heat source in the D2 condenser. In the designed HEN (Liu et al., 2021), the D2 condenser was one of the most vital heat sources in the petrochemical plant, where the temperature was higher than the rest reboilers. As shown in Fig. 2(a), a D2 condenser (corresponding to H3) was used to heat the reboilers of D3-D6 (corresponding to C8, C10, C12, and C13). However, the rest of the hot streams (H4–H6), these streams were cooled directly by the cold utility. Therefore, there is a potential to utilise waste heat by applying an additional ORC. By recovering waste heat, the energy system's efficiency can be increased, and overall energy

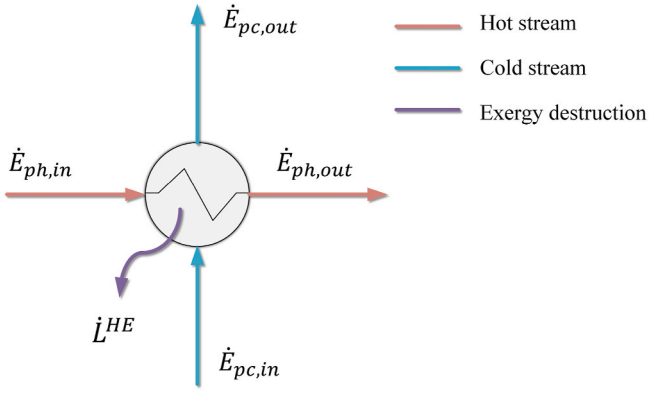

Fig. 4. Flow exergy of the hot and cold streams in a heat exchanger.

Table 1
Economic evaluation assumption.

Parameter	Value
Working hours (Liu et al., 2021)	8000
C_f ($) (Liu et al., 2021)	8000
C_{hu} ($/kW) (Liu et al., 2021)	295
C_{cu} ($/kW) (Liu et al., 2021)	10
Electricity price($/kW•h) (Xu et al., 2020)	0.14
α^{tur} (Xu et al., 2020)	0.67
α^{pump} (Xu et al., 2020)	0.67
C_{tur} ($/kW) (Xu et al., 2020)	6639.70
C_{pump} ($/kW) (Xu et al., 2020)	977.24
i (Liu et al., 2021)	0.1
n (Liu et al., 2021)	5

Table 2
Domain of decision variables.

Variables	Lower bound	Upper bound
T_c (°C)	35	75
T_e (°C)	75	120
m_{wf} (kg/s)	50	120

consumption can be reduced. The designed heat recovery system diagram for the aromatics complex is illustrated in Fig. 2(b). The waste heat directly drove ORC from the streams in HEN. The cold utility could be decreased by adapting an ORC to a heat recovery system. Meanwhile, the ORC could utilise heat to generate electricity as an extra benefit.

The ORC consists of four components, namely the evaporator, turbine, condenser, and pump. As shown in Fig. 3, the working fluid contains different state points, which are also mapped onto the temperature-entropy (T-S) diagram. At point 1, the saturated liquid is pumped to higher pressure at point 2. Then, the hot streams in HEN heat the working fluid in the evaporator. The evaporator contains two sections, preheating (point 2 to point 3) and evaporating (point 3 to point 4) processes. From state point 4, the vapour fluid is expanded in the turbine to low-pressure state point 5. Finally, the working fluid in the condenser is cooled to saturated vapour (point 6) in the precooling section and then to saturated liquid (point 1) in the condensing section. The n-butane was selected as the working fluid.

3. Mathematical modelling and performance analysis methodologies

The mathematical model for the integrated heat recovery system (HEN and ORC) was first developed in this section. Then, the performance of the proposed system was analysed from three perspectives: (1) energy analysis based on the first law of thermodynamics, (2) exergy

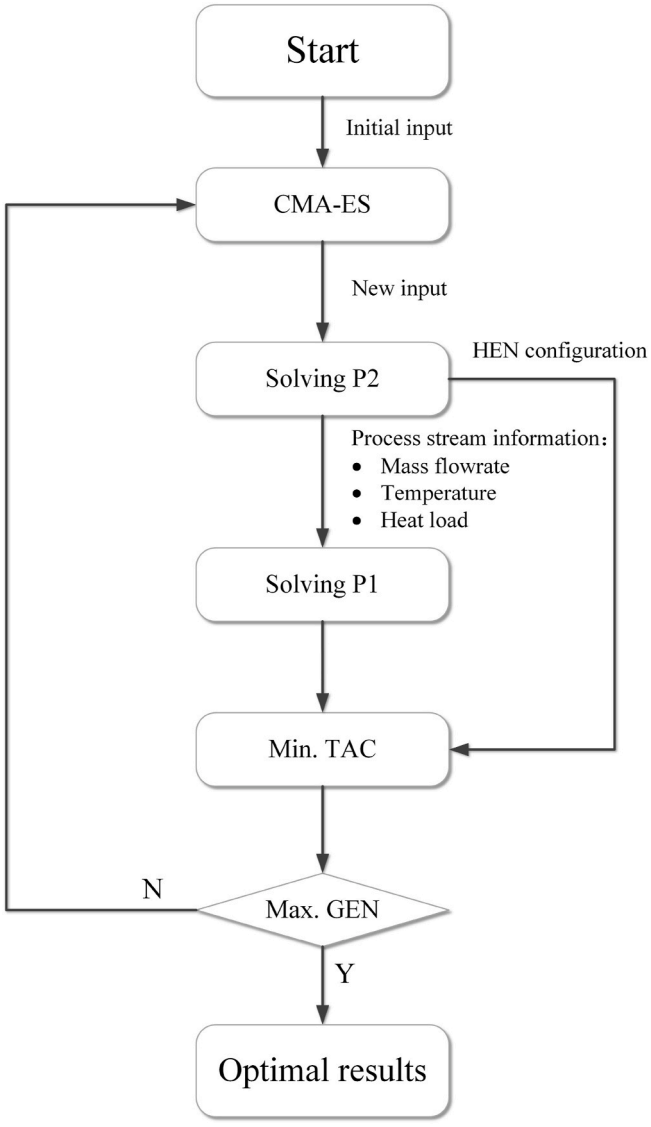

Fig. 5. Flowchart of the optimisation procedure.

analysis by the second law of thermodynamics, and (3) economic analysis. These are typical analysis methodologies for energy systems (Lee and You, 2019). After that, a decomposed strategy was presented to make the mathematical model easier to solve. Finally, steady-state optimisation was performed to obtain the optimal operating conditions for the proposed system. The following assumptions are made to simplify the process (Kouyialis, 2019; Liu et al., 2021; Mehrabadi and Boyaghchi, 2021; Uebbing et al., 2021):

(1) The pressure drops in heat exchangers, including the evaporator and condenser in ORC, are negligible.
(2) The heat losses in various components are negligible.
(3) The working fluid was saturated after the outlet of the evaporator and condenser.
(4) The temperature rise of working fluid across the pump is ignored (i.e. the temperature of state point 2 equals point 1).
(5) The isentropic efficiencies of the pump and turbine are fixed at 70% and 75%, respectively.

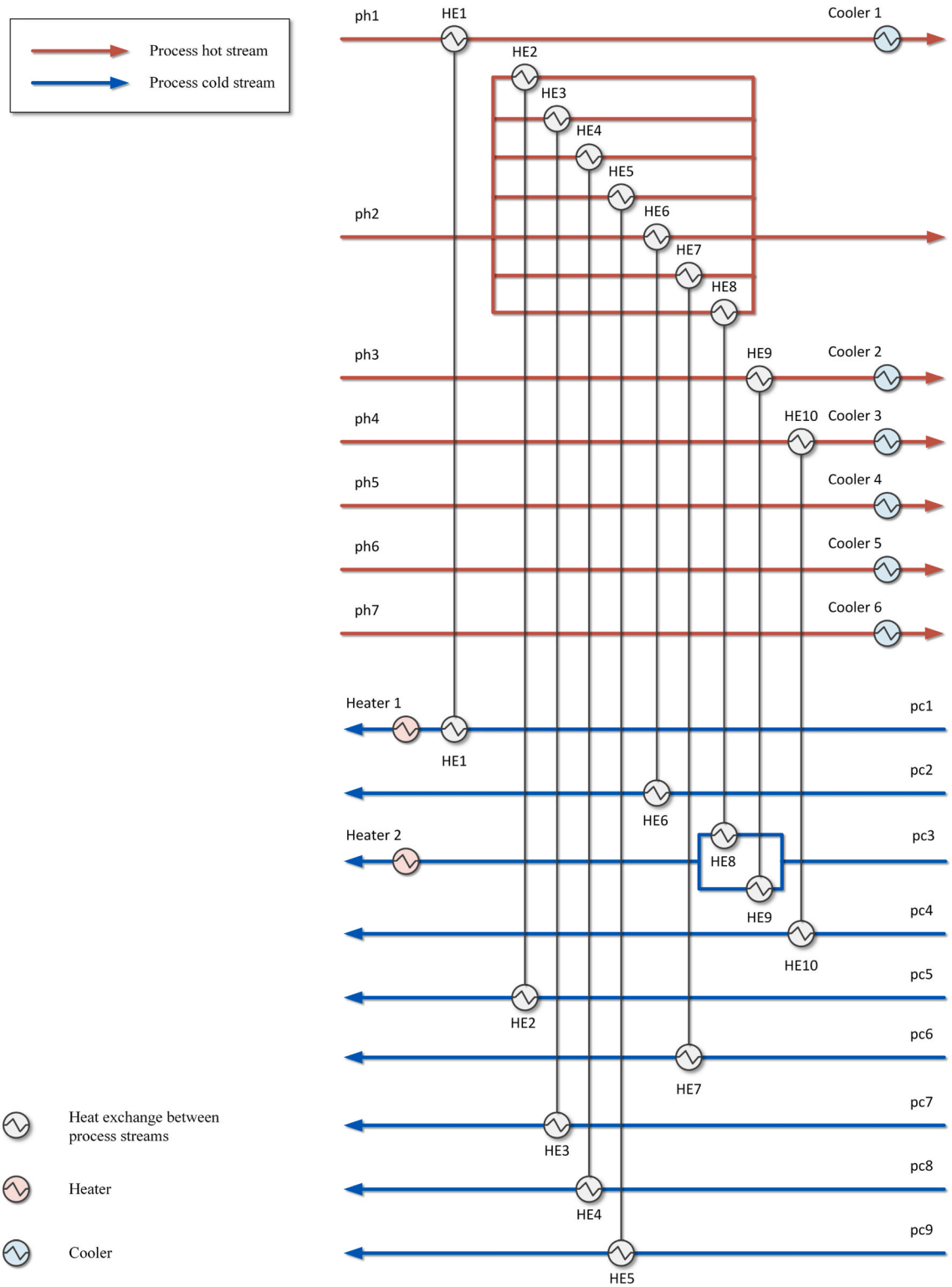

Fig. 6. The HEN configuration for Case 1 (Liu et al., 2021).

3.1. The mathematical model formulation for the proposed heat recovery system

The proposed heat recovery system for the petrochemical plant includes HEN with ORC. One of the purposes of this work is to design the layout of the proposed heat recovery system. It should be noted that the investigated system contains phase-changing process streams. In other words, the original stage-wise superstructure (SWS) model proposed by Yee et al. (Yee et al., 1990a, 1990b; Yee and Grossmann, 1990) is hard to deal with the issue. In addition, the modified stage-wise superstructure (MSWS) proposed by Ponce-Ortega et al. (2008) can tackle the phase-changing streams, but only for small-to medium-scale models. Therefore, an extended mathematical model is developed.

In the developed mathematical model, some simplifications are proposed for the model. The ORC streams were divided into two categories, including non-isothermal and isothermal streams. It is aimed to

Table 3
The detailed information on heat exchangers, heaters, and coolers for Case 1.

Items	Heat load (MW)	Area (m^2)
	Case 1	Case 1
HE1	160.84	13,391.47
HE2	23.07	2185.88
HE3	85.34	13,070.40
HE4	10.59	351.69
HE5	8.48	334.59
HE6	13.41	772.43
HE7	21.82	370.70
HE8	6.28	85.43
HE9	6.64	124.20
HE10	6.41	261.13
Cooler 1	7.48	557.99
Cooler 2	0.88	10.44
Cooler 3	8.05	103.19
Cooler 4	20.66	219.44
Cooler 5	6.05	204.26
Cooler 6	8.12	99.16
Heater 1	8.73	96.21
Heater 2	1.54	8.29
HEphpc	342.88	30,947.92
Total heat exchange	342.88	30,947.92
COOLERph	51.24	1194.48
Total cold utility	51.24	1194.48
HEATERpc	10.27	104.50
Total hot utility	10.27	104.50

Note: *HEphpc* means the heat exchanger for process hot stream and cold stream, *HEphoc* denotes the heat exchanger for process hot stream and ORC cold stream, *COOLERph* represents the cooler used for process hot stream, *COOLERoh* is the cooler used for ORC hot stream, and *HEATERpc* represents the heater used to heat the process cold stream.

reduce the number of binary variables and the model size so that the mathematical model is easier to find the solution than the original one. Meanwhile, constraints were added to prevent the ORC isothermal stream from being heated while the non-isothermal not being heated. The detailed formulations of the extended mathematical model are demonstrated in the supplementary information (*Eqs*. *S*1 − *S*63).

3.2. Performance analysis methodologies

3.2.1. Energy analysis

The energy analysis is applied to the proposed system and each component. The overall heat recovered by the proposed system could be expressed as:

$$\dot{Q}^{Rec} = \sum \dot{Q}^{HE} \tag{1}$$

Where $\dot{Q}$ is the heat flow. The superscripts *Rec* and *HE* denote the recovery and heat exchanger. The energy balance equations for each heat exchanger, heater, and cooler are given in *Eqs*. (S1 − S8). For each component in ORC, the energy balance equations were calculated as:

$$\dot{Q}_{eva}^{ORC} = m_{wf} * (h_5 - h_1) \tag{2}$$

$$\dot{W}_{tur} = m_{wf} * (h_4 - h_5) \tag{3}$$

$$\dot{Q}_{con}^{ORC} = m_{wf} * (h_4 - h_2) \tag{4}$$

$$\dot{W}_{pump} = m_{wf} * (h_2 - h_1) \tag{5}$$

$$\dot{W}_{net} = \dot{W}_{tur} - \dot{W}_{pump} \tag{6}$$

Where *m*, *h*, and $\dot{W}$ are mass flow, enthalpy, and work. The number in the subscript corresponds to the state point in Fig. 3. The subscripts *eva*, *tur*, *con*, *pump*, *wf* and *net* denote the evaporator, turbine, condenser, pump, working fluid, and net value, respectively. The ORC energy efficiency was based on the first law of thermodynamics and defined as (Yağlı et al., 2021):

$$\eta_{ene}^{ORC} = \frac{\dot{W}_{net}}{\dot{Q}_{eva}^{ORC}} \tag{7}$$

Where η represents the efficiency, the superscript *ORC* represents the ORC sub-system, and the subscript *ene* denotes the energy.

3.2.2. Exergy analysis

The exergy efficiency is based on the second law of thermodynamics. It is a useful indicator related to the amount of available energy that can be lost or destructed (Lee and You, 2019). The applied exergy methods are derived from the literature (Yağlı et al., 2021). The physical exergy rate could be expressed as:

$$\dot{E}xg = m * \{(h - h_0) - T_0 * (s - s_0)\} \tag{8}$$

Where $\dot{E}xg$ and *s* denote the exergy rate and entropy. The subscript 0 denotes the atmospheric conditions (25 °C, 1atm).

The exergy destruction and exergy efficiency of each component in ORC were defined as follows:

$$\dot{L}^{eva} = \left(\dot{E}xg_{ph,in} + \dot{E}xg_2\right) - \left(\dot{E}xg_{ph,out} + \dot{E}xg_4\right) \tag{9}$$

$$\eta_{Exg}^{eva} = \frac{\dot{E}xg_4 - \dot{E}xg_2}{\dot{E}xg_{ph,in} - \dot{E}xg_{ph,out}} \tag{10}$$

$$\dot{L}^{tur} = \dot{E}xg_4 - \left(\dot{E}xg_5 + \dot{W}_{tur}\right) \tag{11}$$

$$\eta_{Exg}^{tur} = \frac{\dot{W}_{tur}}{\dot{E}xg_4 - \dot{E}xg_5} \tag{12}$$

$$\dot{L}^{con} = \left(\dot{E}xg_5 + \dot{E}xg_{pc,in}\right) - \left(\dot{E}xg_1 + \dot{E}xg_{pc,out}\right) \tag{13}$$

$$\eta_{Exg}^{con} = \frac{\dot{E}xg_{pc,out} - \dot{E}xg_{pc,in}}{\dot{E}xg_5 - \dot{E}xg_1} \tag{14}$$

$$\dot{L}^{pump} = \left(\dot{E}xg_1 + \dot{W}_{pump}\right) - \dot{E}xg_2 \tag{15}$$

$$\eta_{Exg}^{pump} = \frac{\dot{E}xg_2 - \dot{E}xg_1}{\dot{W}_{pump}} \tag{16}$$

Where $\dot{L}$ is the exergy destruction. The subscripts *ph*, *pc*, and *Exg* denote the process hot stream, process cold stream, and exergy, respectively. The exergy efficiency of the ORC could be derived as:

$$\eta_{Exg}^{ORC} = \frac{\dot{W}_{net}^{ORC}}{\dot{E}xg_{in}^{ORC}} \tag{17}$$

$$\dot{W}_{net}^{ORC} = \dot{W}_{tur} - \dot{W}_{pump} \tag{18}$$

$$\dot{E}xg_{in}^{ORC} = \dot{E}xg_{ph,in}^{eva} - \dot{E}xg_{ph,out}^{eva} \tag{19}$$

As shown in Fig. 4, the exergy destruction and exergy efficiency of each heat exchanger, heater, and cooler could be calculated by (Mehdizadeh-Fard and Pourfayaz, 2018):

$$\dot{L}^{HE} = \left(\dot{E}xg_{ph,in} - \dot{E}xg_{ph,out}\right) + \left(\dot{E}xg_{pc,in} - \dot{E}xg_{pc,out}\right) \#(20.) \tag{20}$$

$$\eta_{Exg}^{HE} = \frac{\dot{E}xg_{pc,out} - \dot{E}xg_{pc,in}}{\dot{E}xg_{ph,in} - \dot{E}xg_{ph,out}} \tag{21}$$

$$\dot{L}^{heater} = \left(\dot{E}xg_{hu,in} - \dot{E}xg_{hu,out}\right) + \left(\dot{E}xg_{pc,in} - \dot{E}xg_{pc,out}\right) \tag{22}$$

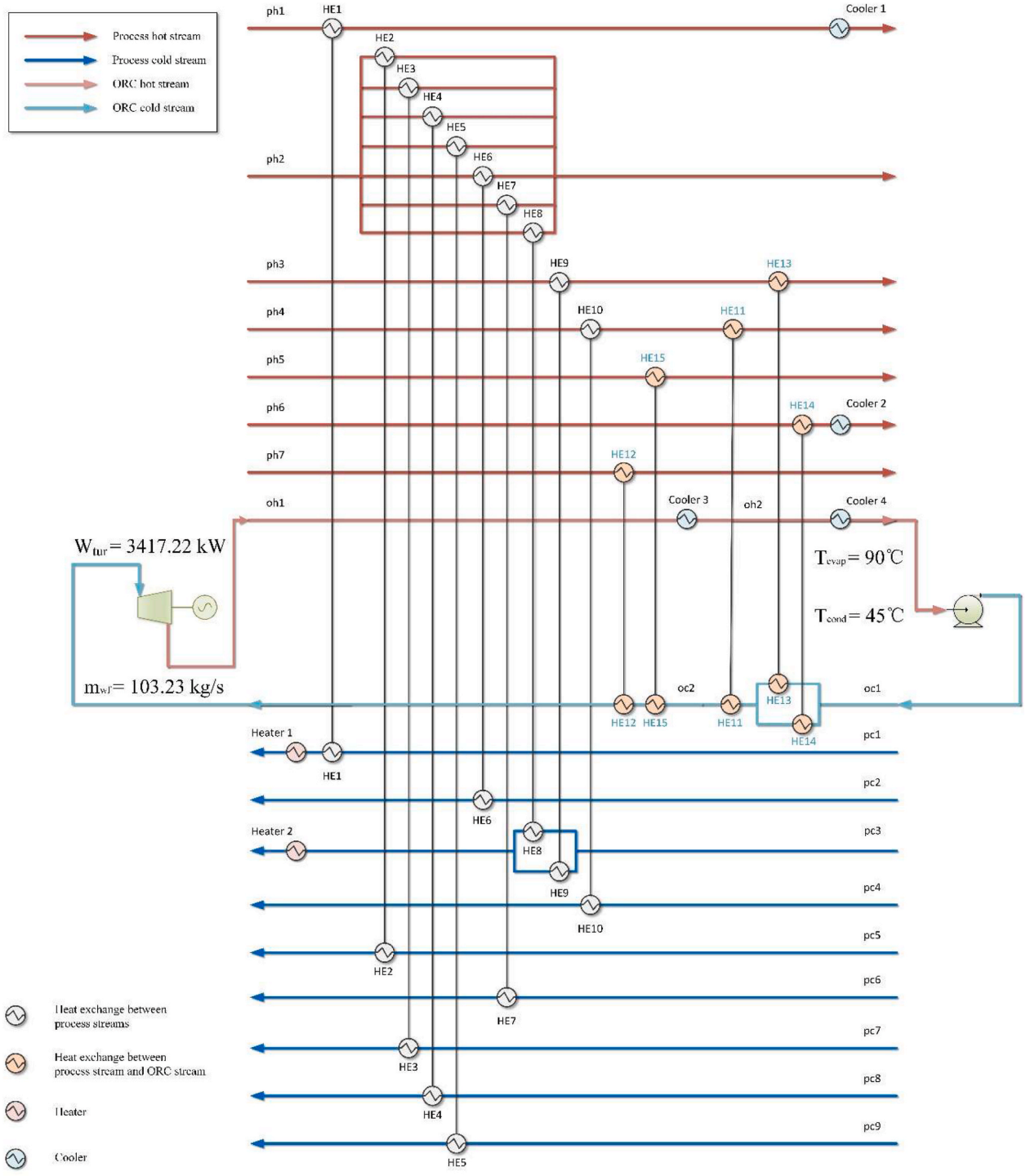

Fig. 7. The HEN and ORC configuration for Case 2.

Table 4
The detailed information on heat exchangers, heaters, and coolers for Case 2.

Items	Heat load (MW)	Area (m^2)
	Case 2	Case 2
HE1	160.84	13,391.47
HE2	23.07	2185.88
HE3	85.34	13,070.40
HE4	10.59	351.69
HE5	8.48	334.59
HE6	13.41	772.43
HE7	21.82	370.70
HE8	6.28	85.43
HE9	6.64	124.20
HE10	6.41	261.13
HE11	8.05	152.17
HE12	8.12	84.29
HE13	0.88	7.10
HE14	4.12	111.39
HE15	20.66	186.16
Cooler 1	7.48	557.99
Cooler 2	1.93	124.36
Cooler 3	2.98	169.25
Cooler 4	35.46	824.76
Heater 1	8.73	96.21
Heater 2	1.54	8.29
HEphpc	342.88	30,947.92
HEphoc	41.83	541.11
Total heat exchange	384.71	31,489.03
COOLERph	9.41	682.35
COOLERoh	38.43	994.01
Total cold utility	47.84	1676.36
HEATERpc	10.27	104.50
Total hot utility	10.27	104.50

Table 5
Key parameters of ORC in Case 2.

Items	Case 2
T_c (°C)	45.00
T_e (°C)	90.00
m_{wf} (kg/s)	103.23
W_{tur} (kW)	3417.22
W_{pump} (kW)	220.40
W_{net} (kW)	3196.82
$\dot{Q}_{con}^{ORC}$ (kW)	38,433.71
$\dot{Q}_{eva}^{ORC}$ (kW)	41,833.94
η_{ene}^{ORC} (%)	7.64

$$\dot{Exg}_{hu,in} - \dot{Exg}_{hu,out} = \int_0^{Q_{hu}} \left(1 - \frac{T_0}{T_{hu}}\right) dQ \tag{23}$$

$$\eta_{Exg}^{heater} = \frac{\dot{Exg}_{pc,out} - \dot{Exg}_{pc,in}}{\dot{Exg}_{hu,in} - \dot{Exg}_{hu,out}} \tag{24}$$

$$\dot{L}^{cooler} = \left(\dot{Exg}_{ph,in} - \dot{Exg}_{ph,out}\right) + \left(\dot{Exg}_{cu,in} - \dot{Exg}_{cu,out}\right) \tag{25}$$

$$\dot{Exg}_{cu,in} - \dot{Exg}_{cu,out} = \int_0^{Q_{cu}} \left(1 - \frac{T_0}{T_{cu}}\right) dQ \tag{26}$$

$$COP^{HEN} = Costhc_{phpc} + Costhc_{phoc} + Costhc_{ohpc} + Costcu_{ph} + Costcu_{oh} + Costhu_{pc} \tag{33}$$

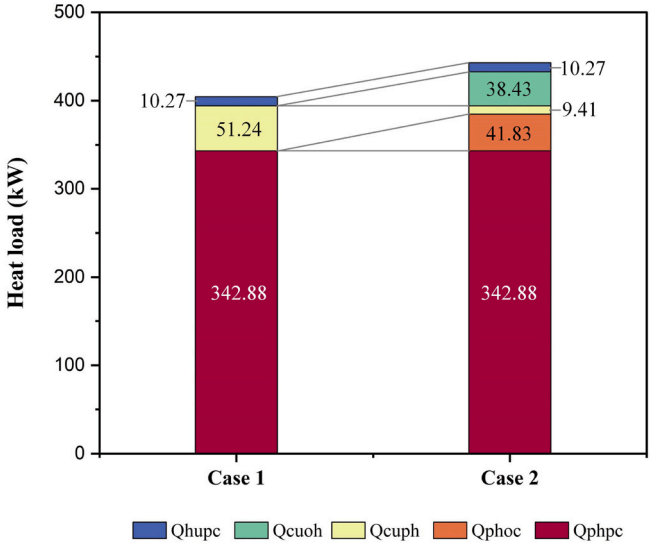

Fig. 8. Heat loads distribution of Case 1 and Case 2.

$$\eta_{Exg}^{cooler} = \frac{\dot{Exg}_{cu,in} - \dot{Exg}_{cu,out}}{\dot{Exg}_{ph,in} - \dot{Exg}_{ph,out}} \tag{27}$$

Where the superscripts *heater* and *cooler* represent the heater and cooler. The subscripts *hu* and *cu* denote the hot utility and cold utility. For the HEN, the total exergy destruction was calculated by summation of all the individual exergy destructions in heat exchangers:

$$\dot{L}^{HEN} = \sum \dot{L}^{HE} + \sum \dot{L}^{heater} + \sum \dot{L}^{cooler} \tag{28}$$

Where the superscript *HEN* denotes the HEN sub-system. The following equations could calculate the total exergy efficiency of the HEN:

$$\eta_{Exg}^{HEN} = \frac{\sum\left(\dot{Exg}_{pc,out} - \dot{Exg}_{pc,in}\right) + \sum\left(\dot{Exg}_{cu,in} - \dot{Exg}_{cu,out}\right)}{\sum\left(\dot{Exg}_{ph,in} - \dot{Exg}_{ph,out}\right) + \sum\left(\dot{Exg}_{hu,in} - \dot{Exg}_{hu,out}\right)} \tag{29}$$

The overall exergy efficiency of the whole energy system was derived as:

$$\eta_{Exg}^{ovrl} = \frac{\sum\left(\dot{Exg}_{pc,out} - \dot{Exg}_{pc,in}\right) + \sum\left(\dot{Exg}_{cu,in} - \dot{Exg}_{cu,out}\right) + \dot{W}_{net}}{\sum\left(\dot{Exg}_{ph,in} - \dot{Exg}_{ph,out}\right) + \sum\left(\dot{Exg}_{hu,in} - \dot{Exg}_{hu,out}\right)} \tag{30}$$

Where the superscript *ovrl* denotes overall. The overall exergy inputs are the exergy flow changes of process hot streams and hot utility, while the overall outputs are the exergy flow changes of process cold streams and cold utility and the power generated by the ORC.

3.2.3. Economic analysis

To investigate the economic feasibility, an economic evaluation was performed. The total annual cost of the proposed system was calculated as follows:

$$TAC = AF * \left(COP^{HEN} + COP^{ORC}\right) + Utility_{cost} - ELE_{profit} \tag{31}$$

$$ELE_{profit} = C_{elec} * \dot{W}_{net} * t_{working} \tag{32}$$

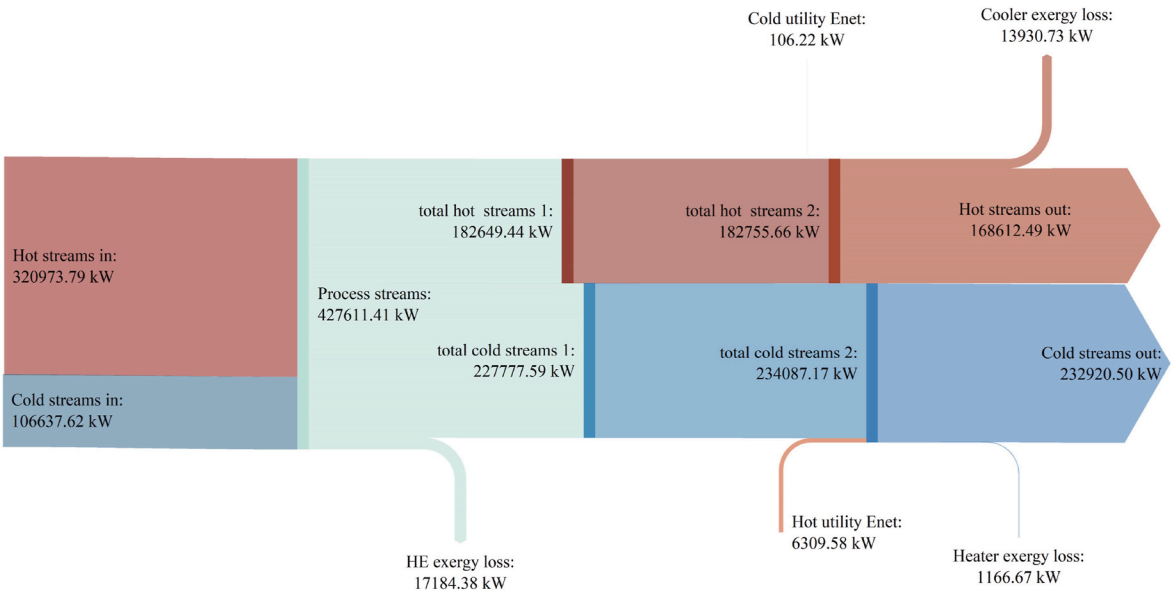

Fig. 9. Exergy flow diagram of Case 1.

Table 6
The exergy destruction of each component for Case 1.

Items	Case 2
$\dot{L}^{HE}$ (HE1)	8283.33
$\dot{L}^{HE}$ (HE2)	1002.86
$\dot{L}^{HE}$ (HE3)	1803.69
$\dot{L}^{HE}$ (HE4)	1128.65
$\dot{L}^{HE}$ (HE5)	726.82
$\dot{L}^{HE}$ (HE6)	824.79
$\dot{L}^{HE}$ (HE7)	2342.72
$\dot{L}^{HE}$ (HE8)	982.26
$\dot{L}^{HE}$ (HE9)	1847.23
$\dot{L}^{HE}$ (HE10)	1001.70
$\dot{L}^{cooler}$ (Cooler 1)	563.65
$\dot{L}^{cooler}$ (Cooler 2)	286.59
$\dot{L}^{cooler}$ (Cooler 3)	1394.13
$\dot{L}^{cooler}$ (Cooler 4)	8046.52
$\dot{L}^{cooler}$ (Cooler 5)	1342.43
$\dot{L}^{cooler}$ (Cooler 6)	2297.41
$\dot{L}^{heater}$ (Heater 1)	821.10
$\dot{L}^{heater}$ (Heater 2)	345.57
$\dot{Exg}_{cu,net}$	106.22
$\dot{Exg}_{hu,net}$	6309.58
$\dot{Exg}_{ph,net}$	152,361.30
$\dot{Exg}_{pc,net}$	126,282.88
η^{ovrl}_{Exg}	79.65%

Note: unit for the exergy destruction is kW.

$$Costhc_{phpc} = \sum_{ph\in PH}\sum_{pc\in PC}\sum_{k\in ST}\left(C_f z_{ph,pc,k} + Area_{ph,pc,k}\right) \tag{34}$$

$$Costhc_{phoc} = \sum_{ph\in PH}\sum_{oc\in OC}\sum_{k\in ST}\left(C_f z_{ph,oc,k} + Area_{ph,oc,k}\right) \tag{35}$$

$$Costhc_{ohpc} = \sum_{oh\in OH}\sum_{pc\in PC}\sum_{k\in ST}\left(C_f z_{oh,pc,k} + Area_{oh,pc,k}\right) \tag{36}$$

$$Costcu_{ph} = \sum_{ph\in PH}\left(C_f zcu_{ph} + Areacu_{ph}\right) \tag{37}$$

$$Costhu_{pc} = \sum_{pc\in PC}\left(C_f zhu_{pc} + Areahu_{pc}\right) \tag{38}$$

$$Costcu_{oh} = \sum_{oh\in OH}\left(C_f zcu_{oh} + Areacu_{oh}\right) \tag{39}$$

$$COP^{ORC} = C_{tur} * \left(\dot{W}_{tur}\right)^{\alpha^{tur}} + C_{pump} * \left(\dot{W}_{pump}\right)^{\alpha^{pump}} \tag{40}$$

$$Utility_{cost} = C_{hu} * \sum_{pc\in PC} qhu_{pc} + C_{cu} * \left(\sum_{ph\in PH} qcu_{ph} + \sum_{oh\in OH} qcu_{oh}\right) \tag{41}$$

$$AF = \frac{i(1+i)^n}{(1+i)^n - 1} \tag{42}$$

where *TAC*, *AF*, *COP*, *Utility*, *ELE*, $t_{working}$, *Costhc*, *Costcu*, *Costhu*, *C*, *Area*, *Areacu*, *Areahu*, *qhu*, *qcu*, α, *i*, and *n* represent the total annual cost, an annual factor, cost of equipment, utility, electricity, working hours, cost of heat exchanger, cooler cost, heater cost, fixed cost, area for HE, area for the cooler, area for the heater, heat load for the heater, heat load for cooler, the parameter for the equipment, fractional interest rate per year, and the horizon time, respectively. Binary variables *z*, *zhu*, and *zcu* denote the existence of HE, heater, and cooler, respectively. The subscripts *oh*, *oc*, and *k* represent ORC hot stream, ORC cold stream, and stage number, respectively. The economic evaluation assumptions are listed in Table 1.

3.3. Decomposed strategy

The model for the design of the layout of the proposed heat recovery system could be formulated as the following problem P1:

P1: *min TAC*

s.t. Eqs. (*S*1 − *S*63), *Eqs.* (32 − 42).

The objective was to minimise the *TAC*. The problem P1 was formulated as the MINLP model. When solving the MINLP model directly, it is hard to converge. Hence, a decomposed strategy was presented to tackle the issue. The problem P1 was decomposed into two sub-problems. The first sub-problem addressed the HEN synthesis

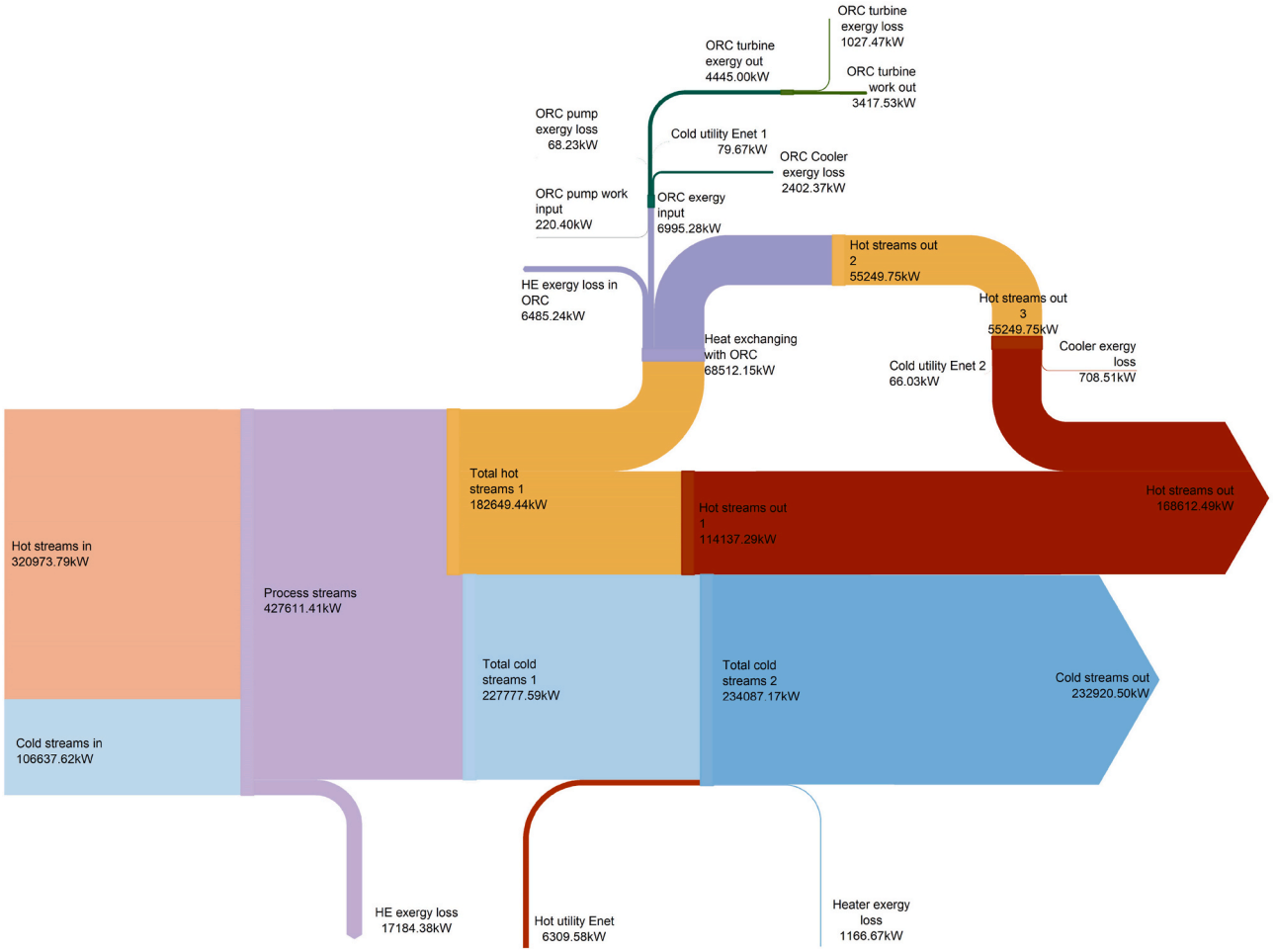

Fig. 10. Exergy flow diagram of Case 2.

among process streams and was formulated as problem P2:

P2: *min TAC*

s.t. Eqs. (*S*1 − *S*4), *Eqs.* (S9 − S10), *Eqs.* (S13 − S14), *Eqs.* (S17 − S20),

Eqs. (S25 − S26), *Eqs.* (S29 − S30), *Eqs.* (S32 − S34), *Eqs.* (S38 − S39),

Eqs. (S44 − S45), *Eqs.* (S47 − S49), *Eqs.* (S52 − S53), *Eqs.* (S58 − S60),

Eq. (35), *Eqs.* (38 − 39), *Eqs.* (41 − 42).

The second sub-problem tackled the synthesis between ORC streams and process streams, which was formulated as the same as problem P1. First, problem P2 was solved, and the matches between process streams were obtained. After that, the streams that need utilities to reach the target temperature were treated as the new process streams in the second sub-problem. Then, the matches between process streams and ORC streams were obtained by solving the second sub-problem. Finally, the layout of the proposed heat recovery system was composed of the matches obtained by solving the two sub-problems. Therefore, compared with solving P1 directly, the decomposed strategy could reduce the model size and make it easier to solve.

3.4. Optimisation procedure

The ORC operating conditions need to be optimised to achieve the minimum *TAC*. The decision variables, including the evaporation temperature (T_e), condensation temperature (T_c) and mass flow rate of the working fluid were considered. These parameters, as well as their reasonable ranges, are listed in Table 2.

The flowchart of the whole optimisation procedure is shown in Fig. 5. First, a set of ORC operation conditions were used as starting points. Then, the new decision variables were generated by the covariance matrix adaptation evolution strategy (CMA-ES) (Hansen et al., 2003). The next step was solving the two sub-problems in sequence. Both sub-problems were formulated as MINLP problems and solved in GAMS 23.8.2. DICOPT was selected as the solver.

Meanwhile, the global solvers BARON and SCIP were also tested. The solution quality that these three solvers provided was similar, but the solution time differed. DICOPT could obtain the solution in 1 s, while the other two solvers need an hour (the maximum execution time is 3600 s). Thus, DICOPT has the advantage in computational efficiency on the premise of similar solution quality when solving the developed model, and is selected as the solver. Finally, it was stopped when the maximum number of iterations was reached (500 iterations) (Liu et al., 2021). The proposed optimisation framework has been automated using MatLab and GAMS (solving the MINLP model in GAMS and the remaining in MatLab R2019a). All optimisation studies were carried out on a PC with an Intel Core i7-8650 CPU at 1.90 GHz and 16.0 GB RAM.

4. Results and discussion

The advantages of the suggested energy system were analysed thermodynamically firstly. Two cases were compared and investigated the efficiency improvement through 3E analysis. The first case (Case 1) only contains the HEN system without ORC, as published in (Liu et al., 2021). It contains 7 hot process streams and 9 cold process streams. The data of process streams and utilities is shown in the supplementary

Table 7
The exergy destruction of each component for Case 2.

Items	Case 2
$\dot{L}^{HE}$ (HE1)	8283.33
$\dot{L}^{HE}$ (HE2)	1002.86
$\dot{L}^{HE}$ (HE3)	1803.69
$\dot{L}^{HE}$ (HE4)	1128.65
$\dot{L}^{HE}$ (HE5)	726.82
$\dot{L}^{HE}$ (HE6)	824.79
$\dot{L}^{HE}$ (HE7)	2342.72
$\dot{L}^{HE}$ (HE8)	982.26
$\dot{L}^{HE}$ (HE9)	1847.23
$\dot{L}^{HE}$ (HE10)	1001.70
$\dot{L}^{HE}$ (HE11)	186.95
$\dot{L}^{HE}$ (HE12)	860.88
$\dot{L}^{HE}$ (HE13)	218.10
$\dot{L}^{HE}$ (HE14)	830.07
$\dot{L}^{HE}$ (HE15)	4391.52
$\dot{L}^{cooler}$ (Cooler 1)	563.65
$\dot{L}^{cooler}$ (Cooler 2)	191.39
$\dot{L}^{cooler}$ (Cooler 3)	246.47
$\dot{L}^{cooler}$ (Cooler 4)	2155.90
$\dot{L}^{heater}$ (Heater 1)	821.10
$\dot{L}^{heater}$ (Heater 2)	345.57
$\dot{L}^{pump}$	68.23
$\dot{L}^{tur}$	1027.47
$\dot{W}_{net}$	3196.82
$\dot{Exg}_{cu,net}$	99.17
$\dot{Exg}_{hu,net}$	6309.58
$\dot{Exg}_{ph,net}$	152,361.30
$\dot{Exg}_{pc,net}$	126,282.90
η^{ovrl}_{Exg}	81.67%

Table 8
Economic evaluation results of Case 1.

Items	Case 1
COP^{HEN} (k$/year)	1363.40
Cost for hot utility (k$/year)	3029.65
Cost for HEN cold utility (k$/year)	512.41
$Utility_{cost}$ (k$/year)	3542.06
TAC (k$/year)	3855.64

Table 9
Economic evaluation results of Case 2.

Items	Case 2
ELE_{profit} (k$/year)	3580.44
COP^{ORC} (k$/year)	1584.08
COP^{HEN} (k$/year)	1498.46
Cost for hot utility (k$/year)	3029.65
Cost for HEN cold utility (k$/year)	94.03
Cost for ORC cold utility (k$/year)	384.34
$Utility_{cost}$ (k$/year)	3508.02
TAC (k$/year)	636.56

information (Table S1). Case 2 consisted of HEN and ORC. Case 2 contained 7 hot process streams, 2 hot ORC steams, 9 cold process streams, and 2 cold ORC steams. The ORC was under fixed operating conditions. The condensing and evaporating temperatures were set to 45 °C and 90 °C. The mass flow rate of the working fluid was fixed at 103.23 kg/s. Then, optimisation was performed based on Case 2, and the optimal case was regarded as Case 3. The results were evaluated through 3E analysis and compared with Case 2.

4.1. Energy analysis

4.1.1. Energy analysis for case 1

Case 1 only contains HEN with 7 hot process streams and 9 cold process streams. The layouts were from Liu et al. (2021), as shown in Fig. 6. The detailed information is given in Table 3.

In Case 1, only process hot stream ph2 did not need cold utility; the rest 6 process hot streams needed a cooler to get the target temperatures. 342.88 MW heat was recovered by HEN. The usage of cold utility was 51.24 MW, and hot utility was 10.27 MW. The results reveal that a large amount of heat is not utilised. There is a potential to recover heat to improve the system efficiency.

4.1.2. Energy analysis for case 2

Case 2 consisted of HEN and ORC. It contained 7 hot process streams, 2 hot ORC steams, 9 cold process streams, and 2 cold ORC steams. Considering that the operating conditions of ORC are fixed, the layouts of Case 2 could be obtained by solving problem P1 and P2 in sequence, as shown in Fig. 7. The detailed information on the layouts is given in Table 4. The key parameters of ORC are shown in Table 5.

In Case 2, only two process hot streams need cold utility, even though increased 2 ORC hot streams need to be cooled directly. By applying ORC to the energy system, 384.17 MW of heat was recovered. Herein, HEN recovered 342.88 MW, and ORC recovered 41.83 MW. The usage of cold utility was 47.84 MW, and hot utility was 10.27 MW. Additionally, the ORC turbine generated 3417.22 kW of power. As calculated by *Eq.* (7), the ORC system efficiency was 7.64%.

4.1.3. Comparison between case 1 and case 2

The heat loads distribution of Case 1 and Case 2 is illustrated in Fig. 8. The main difference is that part of the heat from process streams is used to drive the ORC system. After integrating ORC into HEN, the usage of cold utility for process hot streams decreased from 51.24 MW to 9.41 MW. It corresponds to the decrease in the number of coolers (from 6 to 2) and the increase in the number of heat exchangers (from 10 to 15). The reason is that the decreased 41.83 MW heat is transferred to the working fluid. In addition, the usage of cold utility for ORC hot streams was 38.43 MW in Case 2. Compared with Case 1, the total cold utility usage for Case 2 was 47.84 MW, which decreased by 3.40 MW. Meanwhile, 3196.82 kW of power was generated as extra profit. The data reveals that the investigating energy system could recover more heat and generate extra power.

4.2. Exergy analysis

4.2.1. Exergy analysis for case 1

Fig. 9 shows the exergy flow diagram of Case 1, and the exergy destruction of each component and the overall exergy efficiency are summarised in Table 6. The total exergy loss of heat exchangers, heaters, and coolers was 17,184.38 kW, 1166.67 kW, and 13,930.73 kW, respectively. Notably, the exergy loss of HE1 was the largest. The reason is that the temperature differences and the mass flows are large, and the heat transfer process is irreversible. Additionally, the second exergy destruction occurred in Cooler 4, but the heat load exchanged in HE3 ranks second, which shows two different approaches of the thermodynamics first and second laws analysis in this regard. As calculated by *Eq.* (30), the total exergy efficiency was calculated as 79.65%.

4.2.2. Exergy analysis for case 2

The exergy flow diagram of Case 2 is illustrated in Fig. 10, and the exergy destruction of each component and the overall exergy efficiency are summarised in Table 7. The total exergy destruction of heat exchangers was 23,669.63 kW. The highest exergy destruction occurred in HE1 with 8283.33 kW, and the second exergy destruction occurred in HE15 with 4391.52 kW HE15 could be seen as evaporators in ORC, and used to recover the heat from process hot streams. Apparently, the

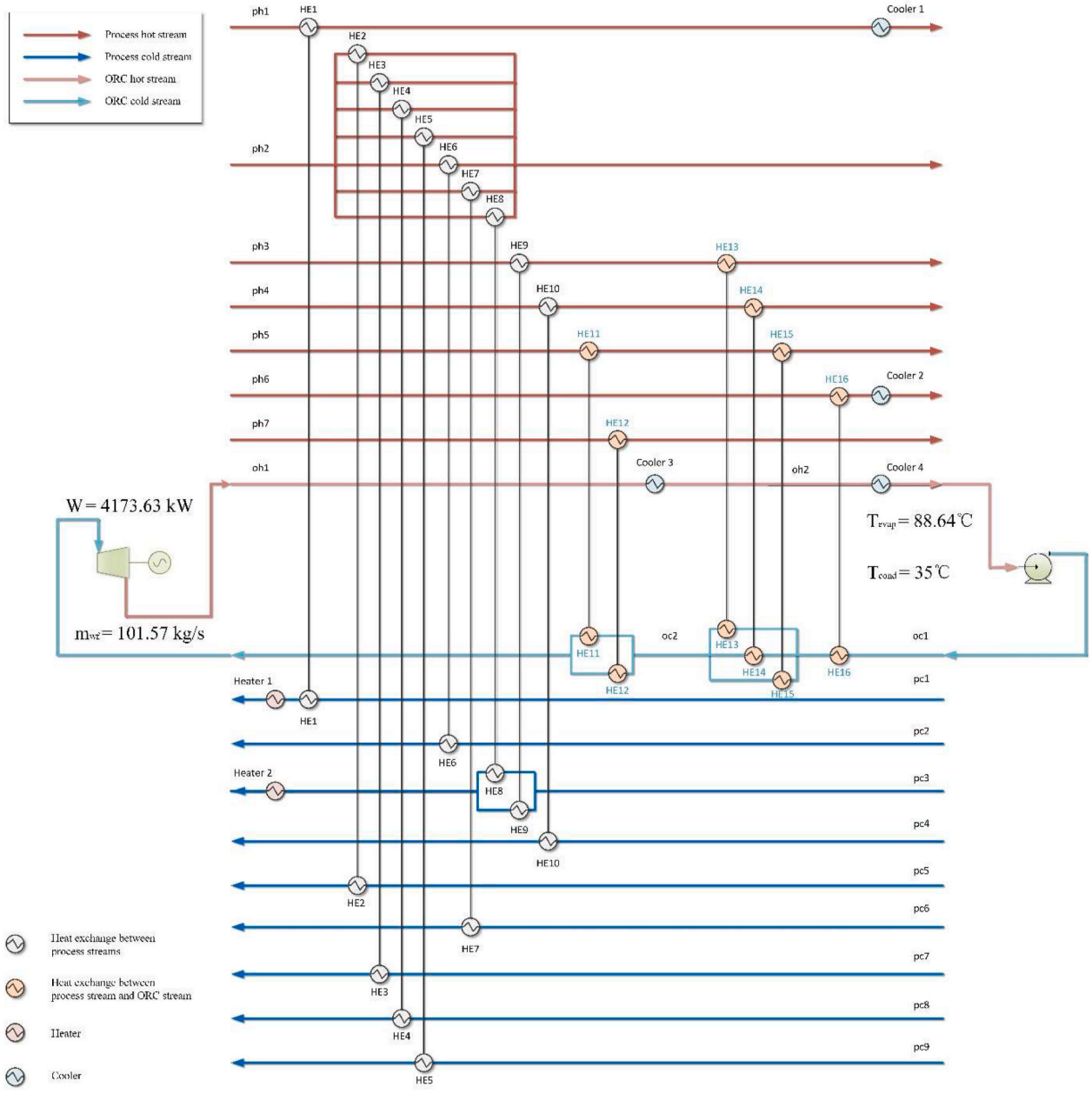

Fig. 11. The HEN and ORC configuration for Case 3.

Table 10
Optimal parameters of ORC for Case 3.

Items	Case 3
T_c (°C)	35.00
T_e (°C)	88.64
m_{wf} (kg/s)	101.57
W_{tur} (kW)	4173.70
W_{pump} (kW)	230.42
W_{net} (kW)	3943.28
$\dot{Q}_{con}^{ORC}$ (kW)	39,417.55
$\dot{Q}_{eva}^{ORC}$ (kW)	43,549.80
η_{ene}^{ORC} (%)	9.05

evaporator's exergy destruction was higher than other components of ORC. Moreover, the total exergy destruction of heaters and coolers was 1166.67 kW and 3157.42 kW, respectively. As calculated by *Eq.* (30), the total exergy efficiency was calculated as 81.67%.

4.2.3. Comparison between case 1 and case 2

After integrating ORC with HEN, the total exergy destruction of heat exchangers rose by 6485.24 kW (from 17,184.38 kW to 23,669.63 kW), and coolers reduced by 10,773.31 kW (from 13,930.73 kW to 3157.42 kW). From the view of the system exergy efficiency, the overall exergy efficiency in Case 2 with 81.67% was 2.01% higher than in Case 1 with 79.65%. The reason is that increasing net power and decreasing cold utility exergy destruction can increase the exergy efficiency. The results show that the suggested energy system has an advantage in exergy efficiency.

Table 11
The detailed information on heat exchangers, heaters, and coolers for Case 3.

Items	Heat load (MW)	Area (m^2)
	Case 3	Case 3
HE1	160.84	13,391.47
HE2	23.07	2185.88
HE3	85.34	13,070.40
HE4	10.59	351.69
HE5	8.48	334.59
HE6	13.41	772.43
HE7	21.82	370.70
HE8	6.28	85.43
HE9	6.64	124.20
HE10	6.41	261.13
HE11	20.45	182.18
HE12	8.12	82.36
HE13	0.88	8.25
HE14	8.05	146.67
HE15	0.21	2.95
HE16	5.84	261.85
Cooler 1	7.48	557.99
Cooler 2	0.21	27.80
Cooler 3	3.43	208.45
Cooler 4	35.99	101.27
Heater 1	8.73	96.21
Heater 2	1.54	8.29
HEphpc	342.88	30,947.92
HEphoc	43.55	684.27
Total heat exchange	386.43	31,370.33
COOLERph	7.69	585.79
COOLERoh	39.42	309.71
Total cold utility	47.11	1697.60
HEATERpc	10.27	104.50
Total hot utility	10.27	104.50

4.3. Economic analysis

4.3.1. Economic analysis for case 1

Table 8 lists the economic evaluation results of Case 1. The cost of hot utility was 3029.65 k$/year, while the cost of cold utility was 512.41 k $/year. The total utility cost was 3542.06 k$/year, which accounts for a large proportion of TAC.

4.3.2. Economic analysis for case 2

The economic evaluation results of Case 2 are shown in Table 9. As integrating ORC into HEN, the extra power was generated by the ORC turbine and brought 3580.44 k$/year profit. The total utility cost was 3508.02 k$/year with 3029.65 k$/year for hot utility and 478.37 k $/year for cold utility. TAC of Case 2 was calculated as 636.56 k$/year.

4.3.3. Comparison between case 1 and case 2

Compared to Case 1, the capital cost of HEN equipment in Case 2 was 135.05 k$/year higher, and the capital cost of ORC equipment was 1584.08 k$/year higher. However, the proposed system in Case 2 could sell electricity as an extra profit (3580.44 k$/year), and the utility cost was lower (decreased by 34.04 k$/year). The TAC value was reduced from 3855.64 k$/year to 636.56 k$/year. In other words, the electricity profit produced by ORC could cover the capital cost of ORC equipment and bring the extra profit simultaneously.

4.4. Optimisation results and 3E analysis

The ORC operation conditions and configuration of the suggested energy system were optimised simultaneously, following optimisation procedure. The optimisation was performed based on Case 2, and the optimal case was regarded as Case 3. The ORC operation conditions in Case 2 were treated as the initial starting points in Case 3.

The optimal configuration of Case 3 is illustrated in Fig. 11. It includes 16 heat exchangers, 2 heaters, and 4 coolers. Compared with Case 1 and Case 2, the layouts of the heat exchangers that transfer heat from process hot streams to cold streams (HE1-HE10) were the same. The reason is that the data of process streams are the same, and the configurations of the heat exchangers are obtained by solving problem P2 with the same solver in GAMS. Furthermore, after optimising the ORC operation conditions, there was one more heat exchanger (HE16) in Case 3, and the sequences of matches were not the same. For stream ph5, it only exchanged heat with oc2 in Case 2, while it exchanged heat with both oc1 and oc2 in Case 3. For stream oc2, it was heated by process hot streams ph5 and ph7 in sequence in Case 2, but in Case 3, it was heated by ph5 and ph7 in parallel. In Case 2, stream oc1 was heated by ph3 and ph6 in parallel first, then heated by ph4. In Case 3, stream oc1 was heated by ph6 first and then by ph3, ph4, and ph5 in parallel. After these arrangements, the matches of HEs in Case 3 could recover more low-grade heat, and the detailed information will be discussed in the energy analysis.

4.4.1. Comparison between case 2 and case 3 based on energy analysis results

The optimal parameters of ORC are shown in Table 10. Based on the equations in Section 3.2, the ORC system efficiency was calculated as 9.05% in Case 3, which was 1.41% higher than in Case 2 (7.64%). In addition, the amount of electricity generated by the turbine in ORC was increased by 22.14%, from 3417.22 kW to 4173.70 kW, while the amount of power used rose by 4.55%, from 220.40 kW to 230.42 kW. The change in the net power generation was a 23.35% increase (from 3196.82 kW to 3943.28 kW). It was directly affected by the decrease in condensing temperature (from 45 °C to 35 °C) and evaporating temperature (from 90.00 °C to 88.64 °C). Notably, the net power increased while the working fluid's mass flow rate decreased (from 103.23 kg/s to 101.57 kg/s). In other words, the net power increase was due not to the increased mass flow rate but to the optimised condensing and evaporating temperature. These results indicate that the performance of the ORC is greater after optimisation.

For the heat exchangers, the detailed information on heat exchangers, heaters, and coolers is listed in Table 11. In the proposed energy system, the low-grade heat recovered by ORC increased by 43.55 MW in Case 3 (1.72 MW more after optimisation). As a result, the total amount of cold utility for process streams decreased (from 9.41 MW to 7.69 MW, respectively), although it was at the cost of increasing the usage of cold utility for ORC cold stream. Moreover, from the view of total heat loads provided by the cold utility, the proposed system saved 4.13 MW of cold utility. These results indicate that the proposed system could recover more heat when the system configuration is optimised simultaneously. Moreover, the optimal ORC operation conditions improved the ORC system performance.

4.4.2. Comparison between case 2 and case 3 based on exergy analysis results

The exergy flow diagram of Case 3 is presented in Fig. 12, and the exergy destruction of each component and the overall exergy efficiency for Case 3 are summarised in Table 12. The overall exergy efficiency of Case 3 was calculated as 82.13%, which was 0.47% higher than Case 2. As calculated in *Eq.*(30), increasing net power and decreasing cold utility exergy destruction would increase the exergy efficiency. As mentioned before, in Case 3, the ORC energy efficiency was best, resulting in the highest net power generated. Additionally, the usage amount of cold utility was the least, which resulted in the least exergy destruction of cold utility. It results in the highest overall exergy efficiency of Case 3.

4.4.3. Comparison between case 2 and case 3 based on economic analysis results

The economic evaluation results of Case 3 are given in Table 13. Compared with Case 2, the electricity profit increased by 836.03 k $/year (from 3580.44 k$/year to 4416.47 k$/year), and the utility cost decreased by 7.32 k$/year, while the cost of HEN and ORC equipment

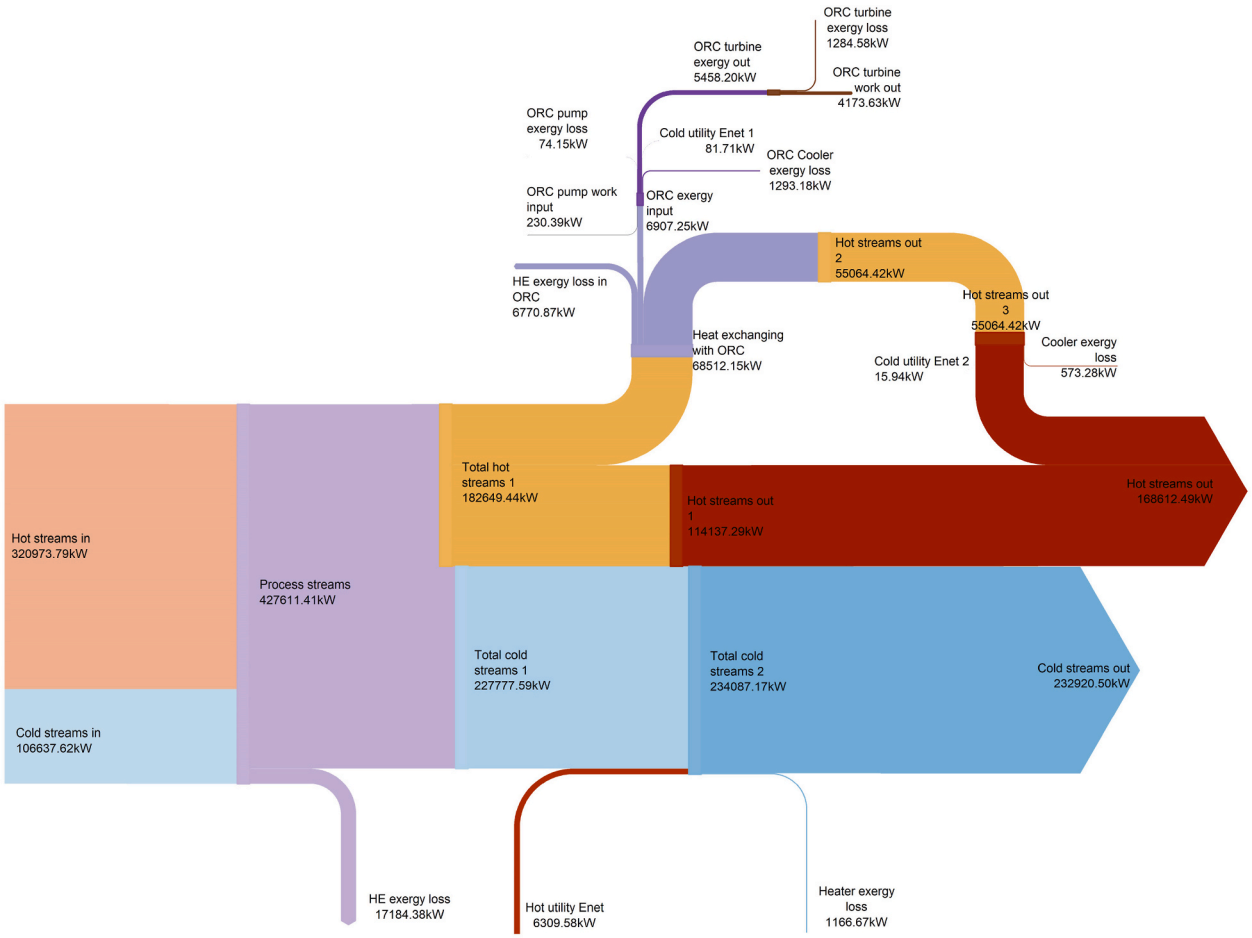

Fig. 12. Exergy flow diagram of Case 3.

Table 12
The exergy destruction of each component for the energy systems of Case 3.

Items	Case 3
$\dot{L}^{HE}$ (HE1)	8283.33
$\dot{L}^{HE}$ (HE2)	1002.86
$\dot{L}^{HE}$ (HE3)	1803.69
$\dot{L}^{HE}$ (HE4)	1128.65
$\dot{L}^{HE}$ (HE5)	726.82
$\dot{L}^{HE}$ (HE6)	824.79
$\dot{L}^{HE}$ (HE7)	2342.72
$\dot{L}^{HE}$ (HE8)	982.26
$\dot{L}^{HE}$ (HE9)	1847.23
$\dot{L}^{HE}$ (HE10)	1001.70
$\dot{L}^{HE}$ (HE11)	4468.01
$\dot{L}^{HE}$ (HE12)	908.98
$\dot{L}^{HE}$ (HE13)	155.31
$\dot{L}^{HE}$ (HE14)	193.19
$\dot{L}^{HE}$ (HE15)	50.46
$\dot{L}^{HE}$ (HE16)	994.92
$\dot{L}^{cooler}$ (Cooler 1)	563.65
$\dot{L}^{cooler}$ (Cooler 2)	9.62
$\dot{L}^{cooler}$ (Cooler 3)	200.21
$\dot{L}^{cooler}$ (Cooler 4)	1092.97
$\dot{L}^{heater}$ (Heater 1)	821.10
$\dot{L}^{heater}$ (Heater 2)	345.57
$\dot{L}^{pump}$	74.15
$\dot{L}^{tur}$	1284.58
$\dot{W}_{net}$	3943.28
$\dot{Exg}_{cu,net}$	97.65
$\dot{Exg}_{hu,net}$	6309.58
$\dot{Exg}_{ph,net}$	152,361.30
$\dot{Exg}_{pc,net}$	126,282.90
η^{ovrl}_{Exg}	82.13%

Table 13
Economic evaluation results of Case 3.

Items	Case 3
ELE_{profit} (k$/year)	4416.47
COP^{ORC} (k$/year)	1807.09
COP^{HEN} (k$/year)	1499.34
Cost for hot utility (k$/year)	3029.65
Cost for HEN cold utility (k$/year)	76.87
Cost for ORC cold utility (k$/year)	394.18
$Utility_{cost}$ (k$/year)	3500.70
TAC (k$/year)	−155.30

increased from 3082.54 k$/year to 3306.44 k$/year. The TAC in Case 3 was 791.86 k$/year less than in Case 2. Therefore, these results reveal that the optimised low-grade recovery system is more profitable than Case 2.

5. Conclusions

This paper presented the study on integrating HEN and ORC for the petrochemical plant to recover the low-grade heat. For the model development of the petrochemical plant, the study first addressed that no documented mathematical model can directly address medium-scale problems involving the majority of phase-changing process streams. The extended MINLP models of HEN and ORC were then developed in GAMS. Three cases were analysed for petrochemical plant with or without the ORC. The system's performance investigation and economic evaluation at design conditions were carried out. The main conclusions are summarised as follows:

Through the 3E analysis, the results show that the suggested system performs better than HEN only (Case 2 vs Case 1), including recovering more heat (increased by 41.83 MW), higher exergy efficiency (increased by 2.01%), and less TAC (decreased by 3219.08 k$/year). Furthermore, optimisation was performed to improve the proposed system by simultaneously optimising the ORC operating conditions and configuration. To simplify the resolution of the model, a decomposition method was employed. The optimisation results indicate that the system performs better under the ORC operation conditions of 35 °C of condensing temperature, 88.64 °C of evaporating temperature, and 101.57 kg/s of ORC working fluid mass flow rate, respectively. Compared Case 3 with Case 2, the optimised system (Case 3) could recover 43.55 MW more heat from the process streams and generate 4416.47 k$/year extra profit. The exergy efficiency of case 3 has risen from 79.65% to 82.13%. These results suggest the advantages by integrating with ORC and HEN. The suggested system could be an effective and promising approach for energy savings for a petrochemical plant. This study was expected to provide a guide to the petrochemical industry needing to be retrofitted or to a new plant. In our future research, the main directions will focus on: 1) Considering the pressure drop when modelling, 2) Integrating the heat recovery system into the petrochemical process and optimising simultaneously.

CRediT authorship contribution statement

Yurong Liu: Conceptualization, Methodology, Software, Validation, Visualization, Formal analysis, Writing – original draft. **Minglei Yang:** Conceptualization, Resources, Investigation, Supervision. **Yuxing Ding:** Conceptualization, Methodology, Software, Validation, Visualization, Formal analysis, Writing – review & editing. **Meihong Wang:** Conceptualization, Resources, Funding acquisition, Supervision, Project administration, Writing – review & editing. **Feng Qian:** Conceptualization, Investigation, Resources, Supervision, Project administration.

Data availability

Data will be made available on request.

Acknowledgement

This work was supported by National Natural Science Foundation of China (Basic Science Center Program: 61988101), International (Regional) Cooperation and Exchange Project (61720106008), National Natural Science Fund for Distinguished Young Scholars (61925305), Fundamental Research Funds for the Central Universities and Shanghai AI Lab. The UK authors would like to acknowledge the financial support of the EU RISE project OPTIMAL (Ref: 101007963).

Appendix B. Supplementary data

Supplementary data to this article can be found online at https://doi.org/10.1016/j.jclepro.2022.135133.

Appendix A. Supplementary data

The following is the Supplementary data to this article:

References

Adibhatla, S., Kaushik, S.C., 2017. Energy, exergy and economic (3E) analysis of integrated solar direct steam generation combined cycle power plant. Sustain. Energy Technol. Assessments 20, 88–97. https://doi.org/10.1016/j.seta.2017.01.002.

Algieri, A., Morrone, P., 2012. Comparative energetic analysis of high-temperature subcritical and transcritical Organic Rankine Cycle (ORC). A biomass application in

the Sibari district. Appl. Therm. Eng. 36, 236–244. https://doi.org/10.1016/j.applthermaleng.2011.12.021.
Altun, A.F., Kilic, M., 2020. Thermodynamic performance evaluation of a geothermal ORC power plant. Renew. Energy 148, 261–274. https://doi.org/10.1016/j.renene.2019.12.034.
Aneke, M., Agnew, B., Underwood, C., 2011. Performance analysis of the Chena binary geothermal power plant. Appl. Therm. Eng. 31, 1825–1832. https://doi.org/10.1016/j.applthermaleng.2011.02.028.
Aneke, M., Agnew, B., Underwood, C., Wu, H., Masheiti, S., 2012. Power generation from waste heat in a food processing application. Appl. Therm. Eng. 36, 171–180. https://doi.org/10.1016/j.applthermaleng.2011.12.023.
Boyaghchi, F.A., Heidarnejad, P., 2015. Thermoeconomic assessment and multi objective optimization of a solar micro CCHP based on Organic Rankine Cycle for domestic application. Energy Convers. Manag. 97, 224–234. https://doi.org/10.1016/j.enconman.2015.03.036.
Bruno, J.C., Lopez-Villada, J., Letelier, E., Romera, S., Coronas, A., 2008. Modelling and optimisation of solar organic rankine cycle engines for reverse osmosis desalination. Appl. Therm. Eng. 28, 2212–2226. https://doi.org/10.1016/j.applthermaleng.2007.12.022.
Campana, F., Bianchi, M., Branchini, L., De Pascale, A., Peretto, A., Baresi, M., Fermi, A., Rossetti, N., Vescovo, R., 2013. ORC waste heat recovery in European energy intensive industries: energy and GHG savings. Energy Convers. Manag. 76, 244–252. https://doi.org/10.1016/j.enconman.2013.07.041.
Chen, C.-L., Li, P.-Y., Le, S.N.T., 2016a. Organic Rankine cycle for waste heat recovery in a refinery. Ind. Eng. Chem. Res. 55, 3262–3275. https://doi.org/10.1021/acs.iecr.5b03381.
Chen, C.-L., Li, P.-Y., Si Nguyen Tien, L., 2016b. Organic rankine cycle for waste heat recovery in a refinery. Ind. Eng. Chem. Res. 55, 3262–3275. https://doi.org/10.1021/acs.iecr.5b03381.
Chen, T., Zhang, B., Chen, Q., 2014. Heat integration of fractionating systems in para-xylene plants based on column optimization. Energy 72, 311–321. https://doi.org/10.1016/j.energy.2014.05.039.
Cioccolanti, L., Hamedani, S.R., Villarini, M., 2019. Environmental and energy assessment of a small-scale solar Organic Rankine Cycle trigeneration system based on Compound Parabolic Collectors. Energy Convers. Manag. 198, 111829 https://doi.org/10.1016/j.enconman.2019.111829.
Daghigh, R., Shafieian, A., 2016. An investigation of heat recovery of submarine diesel engines for combined cooling, heating and power systems. Energy Convers. Manag. 108, 50–59. https://doi.org/10.1016/j.enconman.2015.11.004.
Ding, Y., Olumayegun, O., Chai, Y., Liu, Y., Wang, M., 2022. Simulation, energy and exergy analysis of compressed air energy storage integrated with organic Rankine cycle and single effect absorption refrigeration for trigeneration application. Fuel 317, 123291. https://doi.org/10.1016/j.fuel.2022.123291.
DiPippo, R., 2012. Geothermal Power Plants: Principles, Applications, Case Studies and Environmental Impact. Butterworth-Heinemann.
Drescher, U., Brüggemann, D., 2007. Fluid selection for the Organic Rankine Cycle (ORC) in biomass power and heat plants. Appl. Therm. Eng. 27, 223–228. https://doi.org/10.1016/j.applthermaleng.2006.04.024.
Fergani, Z., Touil, D., Morosuk, T., 2016. Multi-criteria exergy based optimization of an Organic Rankine Cycle for waste heat recovery in the cement industry. Energy Convers. Manag. 112, 81–90. https://doi.org/10.1016/j.enconman.2015.12.083.
Freeman, J., Hellgardt, K., Markides, C.N., 2015. An assessment of solar-powered organic Rankine cycle systems for combined heating and power in UK domestic applications. Appl. Energy 138, 605–620. https://doi.org/10.1016/j.apenergy.2014.10.035.
Ghasemi, H., Paci, M., Tizzanini, A., Mitsos, A., 2013. Modeling and optimization of a binary geothermal power plant. Energy 50, 412–428. https://doi.org/10.1016/j.energy.2012.10.039.
Gökgedik, H., Yürüsoy, M., Kecebas, A., 2016. Improvement potential of a real geothermal power plant using advanced exergy analysis. Energy 112, 254–263. https://doi.org/10.1016/j.energy.2016.06.079.
Hansen, N., Müller, S.D., Koumoutsakos, P., 2003. Reducing the time complexity of the derandomized evolution strategy with covariance matrix adaptation (CMA-ES). Evol. Comput. 11, 1–18. https://doi.org/10.1162/106365603321828970.
Hoang, A.T., 2018. Waste heat recovery from diesel engines based on Organic Rankine Cycle. Appl. Energy 231, 138–166. https://doi.org/10.1016/j.apenergy.2018.09.022.
Horst, T.A., Rottengruber, H.-S., Seifert, M., Ringler, J., 2013. Dynamic heat exchanger model for performance prediction and control system design of automotive waste heat recovery systems. Appl. Energy 105, 293–303. https://doi.org/10.1016/j.apenergy.2012.12.060.
Jung, H.-C., Krumdieck, S., Vranjes, T., 2014. Feasibility assessment of refinery waste heat-to-power conversion using an organic Rankine cycle. Energy Convers. Manag. 77, 396–407. https://doi.org/10.1016/j.enconman.2013.09.057.
Kaska, O., 2014. Energy and exergy analysis of an organic Rankine for power generation from waste heat recovery in steel industry. Energy Convers. Manag. 77, 108–117. https://doi.org/10.1016/j.enconman.2013.09.026.
Kermani, M., Wallerand, A.S., Kantor, I.D., Marechal, F., 2018. Generic superstructure synthesis of organic Rankine cycles for waste heat recovery in industrial processes. Appl. Energy 212, 1203–1225. https://doi.org/10.1016/j.apenergy.2017.12.094.
Kouyialis, G., 2019. Symmetry and Degeneracy in Nonconvex Optimisation Problems : Application to Heat Recovery Networks.
Lee, I., You, F.Q., 2019. Systems design and analysis of liquid air energy storage from liquefied natural gas cold energy. Appl. Energy 242, 168–180. https://doi.org/10.1016/j.apenergy.2019.03.087.
Lion, S., Vlaskos, I., Taccani, R., 2020. A review of emissions reduction technologies for low and medium speed marine Diesel engines and their potential for waste heat recovery. Energy Convers. Manag. 207, 112553 https://doi.org/10.1016/j.enconman.2020.112553.
Liu, Y., Ding, Y., Yang, M., Peng, B., Qian, F., 2022. A trigeneration application based on compressed air energy storage integrated with organic Rankine cycle and absorption refrigeration: Multi-objective optimisation and energy, exergy and economic analysis. J. Energy Storage 55, 105803. https://doi.org/10.1016/j.est.2022.105803.
Liu, Y., Yang, M., Zhao, L., Du, W., Zhong, W., Qian, F., 2021. Simultaneous optimization and heat integration of an aromatics complex with a surrogate model. Ind. Eng. Chem. Res. 60, 3633–3647. https://doi.org/10.1021/acs.iecr.0c05507.
Maraver, D., Royo, J., 2017. Efficiency enhancement in existing biomass organic Rankine cycle plants by means of thermoelectric systems integration. Appl. Therm. Eng. 119, 396–402. https://doi.org/10.1016/j.applthermaleng.2017.03.077.
Mehdizadeh-Fard, M., Pourfayaz, F., 2019. Advanced exergy analysis of heat exchanger network in a complex natural gas refinery. J. Clean. Prod. 206, 670–687. https://doi.org/10.1016/j.jclepro.2018.09.166.
Mehdizadeh-Fard, M., Pourfayaz, F., 2018. A simple method for estimating the irreversibly in heat exchanger networks. Energy 144, 633–646. https://doi.org/10.1016/j.energy.2017.11.158.
Mehrabadi, Z.K., Boyaghchi, F.A., 2021. Exergoeconomic and exergoenvironmental analyses and optimization of a new low-CO2 emission energy system based on gasification-solid oxide fuel cell to produce power and freshwater using various fuels. Sustain. Prod. Consum. 26, 782–804. https://doi.org/10.1016/j.spc.2020.12.041.
Meyers, R.A., 2004. Handbook of Petroleum Refining Processes. McGraw-Hill, New York.
Moreira, L.F., Arrieta, F.R.P., 2019. Thermal and economic assessment of organic Rankine cycles for waste heat recovery in cement plants. Renew. Sustain. Energy Rev. 114, 109315 https://doi.org/10.1016/j.rser.2019.109315.
Papoulias, S.A., Grossmann, I.E., 1983a. A structural optimization approach in process synthesis-I. Utility systems. Comput. Chem. Eng. 7, 695–706. https://doi.org/10.1016/0098-1354(83)85022-4.
Papoulias, S.A., Grossmann, I.E., 1983b. A structural optimization approach in process synthesis-II. Heat recovery networks. Comput. Chem. Eng. 7, 707–721. https://doi.org/10.1016/0098-1354(83)85023-6.
Papoulias, S.A., Grossmann, I.E., 1983c. A structural optimization approach in process synthesis-III. Total processing systems. Comput. Chem. Eng. 7, 723–734. https://doi.org/10.1016/0098-1354(83)85024-8.
Ponce-Ortega, J.M., Jimenez-Gutierrez, A., Grossmann, I.E., 2008. Optimal synthesis of heat exchanger networks involving isothermal process streams. Comput. Chem. Eng. 32, 1918–1942. https://doi.org/10.1016/j.compchemeng.2007.10.007.
Psaltis, A., Sinoquet, D., Pagot, A., 2016. Systematic optimization methodology for heat exchanger network and simultaneous process design. Comput. Chem. Eng. 95, 146–160. https://doi.org/10.1016/j.compchemeng.2016.09.013.
Reddy, C.C.S., Naidu, S.V., Rangaiah, G.P., 2013. Waste heat recovery methods and technologies. Chem. Eng. (United States) 120, 28–38.
Ringler, J., Seifert, M., Guyotot, V., Hübner, W., 2009. Rankine cycle for waste heat recovery of IC engines. SAE Int. J. Engines 2, 67–76.
Shahandeh, H., Ivakpour, J., Kasiri, N., 2014. Internal and external HIDiCs (heat-integrated distillation columns) optimization by genetic algorithm. Energy 64, 875–886. https://doi.org/10.1016/j.energy.2013.10.042.
Song, J., Li, Y., Gu, C., Zhang, L., 2014. Thermodynamic analysis and performance optimization of an ORC (Organic Rankine Cycle) system for multi-strand waste heat sources in petroleum refining industry. Energy 71, 673–680. https://doi.org/10.1016/j.energy.2014.05.014.
Sonsaree, S., Asaoka, T., Jiajitsawat, S., Aguirre, H., Tanaka, K., 2018. A small-scale solar Organic Rankine Cycle power plant in Thailand: three types of non-concentrating solar collectors. Sol. Energy 162, 541–560. https://doi.org/10.1016/j.solener.2018.01.038.
Świerzewski, M., Kalina, J., 2020. Optimisation of biomass-fired cogeneration plants using ORC technology. Renew. Energy 159, 195–214. https://doi.org/10.1016/j.renene.2020.05.155.
Tańczuk, M., Ulbrich, R., 2013. Implementation of a biomass-fired co-generation plant supplied with an ORC (Organic Rankine Cycle) as a heat source for small scale heat distribution system-A comparative analysis under Polish and German conditions. Energy 62, 132–141. https://doi.org/10.1016/j.energy.2013.09.044.
Uebbing, J., Biegler, L.T., Rihko-struckmann, L., Sager, S., Sundmacher, K., 2021. Optimization of pressure swing adsorption via a trust-region filter algorithm and equilibrium theory. Comput. Chem. Eng. 151, 107340 https://doi.org/10.1016/j.compchemeng.2021.107340.
Xu, Y., Wang, L., Chen, Y., Ye, S., Huang, W., 2020. Simultaneous optimization method for directly integrating ORC with HEN to achieve exergy-economy multiobjective. Ind. Eng. Chem. Res. 59, 21488–21501. https://doi.org/10.1021/acs.iecr.0c04039.

Yaglı, H., Koc, Y., Kalay, H., 2021. Optimisation and exergy analysis of an organic Rankine cycle (ORC) used as a bottoming cycle in a cogeneration system producing steam and power. Sustain. Energy Technol. Assessments 44, 100985. https://doi.org/10.1016/j.seta.2020.100985.

Yari, M., Mehr, A.S., Zare, V., Mahmoudi, S.M.S., Rosen, M.A., 2015. Exergoeconomic comparison of TLC (trilateral Rankine cycle), ORC (organic Rankine cycle) and Kalina cycle using a low grade heat source. Energy 83, 712–722. https://doi.org/10.1016/j.energy.2015.02.080.

Yee, T.F., Grossmann, I.E., 1990. Simultaneous optimization models for heat integration–II. Heat exchanger network synthesis. Comput. Chem. Eng. 14, 1165–1184. https://doi.org/10.1016/0098-1354(90)85010-8.

Yee, T.F., Grossmann, I.E., Kravanja, Z., 1990a. Simultaneous optimization models for heat integration–I. Area and energy targeting and modeling of multi-stream exchangers. Comput. Chem. Eng. 14, 1151–1164. https://doi.org/10.1016/0098-1354(90)85009-Y.

Yee, T.F., Grossmann, I.E., Kravanja, Z., 1990b. Simultaneous optimization models for heat integration–III. Process and heat exchanger network optimization. Comput. Chem. Eng. 14, 1185–1200. https://doi.org/10.1016/0098-1354(90)80001-R.

Zhang, B.J., Luo, X.L., Liu, K., Chen, Q.L., Li, W., 2014. Simultaneous target of HEN and columns with variable feed temperatures for a toluene disproportionation plant. Ind. Eng. Chem. Res. 53, 10429–10438. https://doi.org/10.1021/ie500111z.